2. Magnetization distribution in superconducting domains subject to time varying external magnetic field - The equivalent magnetic network

Introduction

In this chapter we describe the model of the equivalent magnetic network, that is an integral method to deal with general magnetoquasistatic problems, which is alternative to the model of the equivalent electric network presented in chapter 1. The basic difference is the characterization of the material, in fact, following this approach, the magnetic response of the superconductor is envisioned as produced by an induced magnetization rather than an induced current.

In section 2.1 the mathematical description of the field problem, based on the Clebsh decomposition of the magnetic field, is given. The expression of the global vector magnetic potential (due to the currents and the magnetization) is also introduced in order to allow a simple statement of the boundary conditions. In section 2.2 the discretization technique of the field problem and its circuit interpretation are described. Numerical details yet developed in chapter 1 are not repeated but appropriate cross references are provided. Specific numerical issues are discussed. In section 2.3 a model to reproduce the hysteresis curves of the superconductor, which serve as constitutive relation, is developed. In section 3.4 the pulsed magnetization process of a superconducting ring is analyzed by means of its equivalent magnetic network. The limits of the equivalence among current and magnetization based models are discussed.

2.1 The mathematical formulation

A fundamental characteristic of the superconductors is their ability to expel the magnetic flux from inside when they are subject to an external imposed magnetic field; this property is referred to as *Meissner effect* and can be conveniently envisioned as resulting from induced currents which flow in a thin layer located by the boundary. These currents create a magnetic field which is equal and opposite to that which is applied in a way to maintain the condition of zero magnetic flux density deep within the material. However, it is not possible to measure such currents; their presence can only be indirectly deduced by measuring the magnetic field distribution outside the superconducting region.

As we know, however, electric currents are not the only possible source of magnetism; fields can also be produced by magnetic moments either induced or intrinsic to a material [32,33]. Therefore, if we agree to restrict ourselves to measurements outside a superconductor, we can envision the field responsible for flux expulsion from inside as produced by a distribution of magnetization which take place within the superconducting material. These distribution affects the field outside in exactly the same way as the currents which give account of the flux expulsion, therefore, by only measuring the magnetic field distribution outside the superconducting region it is not possible to discern whether the reaction field is produced by one or the other source.

Let us consider a system made of a superconducting domain with no transport current and subject to a time varying magnetic field produced by currents flowing in a normal conducting region. The two domains do not intersect each other. Let us assume that no free currents circulate inside the considered superconducting domain and choose to model the flux expulsion property by means of an induced magnetization. We limit our analysis to the cases for which the *magnetoquasistatic* approximation, as defined in section 1.1, holds, i. e. we consider only systems where the magnetic field produced by the currents of the normal conducting domain changes on characteristic time scales which are low enough compared with the time required by an electromagnetic wave to propagate over the entire extension of the system.

The constitutive relation of a material which shows and induced magnetization can be expressed at any point by

$$\mathbf{B}(\mathbf{x},t) = \mu_0 \left(\mathbf{H}(\mathbf{x},t) + \mathbf{M}(\mathbf{x},t)\right) \tag{2.1.1}$$

where vector **M** represents the local density of induced magnetic dipole moments inside the material and depends on the magnetic field **H** by means of a relation which is, in the most general case, non linear and hysteretic and can be expressed as

$$\mathbf{M}(\mathbf{x},t) = \mathcal{M}_H\left(\mathbf{H}(\mathbf{x},\tau), \tau \le t\right) \tag{2.1.2}$$

The condition $\tau \le t$ points out the dependence of the magnetization on the past history of the magnetic field. Function $\mathcal{M}_H$ depends also on the temperature. Equations (2.1.2) and (2.1.1) establish an implicit link between the magnetization **M** and the magnetic flux density **B** which is still non linear and hysteretic and can be expressed as

$$\mathbf{M}(\mathbf{x},t) = \mathcal{M}_B\left(\mathbf{B}(\mathbf{x},\tau), \tau \le t\right) \tag{2.1.3}$$

The magnetic field **H** at any point of the considered system is instantaneously related to the local current density **J** through the Ampere law; since in our model no free currents can circulate inside the superconducting domain it can be expressed as

$$\nabla \times \mathbf{H}(\mathbf{x},t) = \mathbf{J}^{ext}(\mathbf{x},t) \tag{2.1.4}$$

where $\mathbf{J}^{ext}$ represents the current distribution outside the superconductor. Moreover, the magnetic flux density **B** is a solenoidal vector every where, i.e.

$$\nabla \cdot \mathbf{B}(\mathbf{x},t) = 0 \tag{2.1.5}$$

By substituting equation (2.1.1) in equation (2.1.5) it follows

$$\nabla \cdot \mathbf{H}(\mathbf{x},t) = -\nabla \cdot \mathbf{M}(\mathbf{x},t) \tag{2.1.6}$$

Equations (2.1.6) and (2.1.4) show that there are two possible sources for the magnetic field in the considered system: the magnetization inside the superconductor and the currents which circulate outside.

Let us now introduce two components $\mathbf{H}_J$ and $\mathbf{H}_M$ of magnetic field subject to the following conditions

$$\nabla \times \mathbf{H}_J(\mathbf{x},t) = \mathbf{J}^{ext}(\mathbf{x},t) \tag{2.1.7}$$

$$\nabla \cdot \mathbf{H}_J(\mathbf{x},t) = 0 \tag{2.1.8}$$

and

$$\nabla \times \mathbf{H}_M(\mathbf{x},t) = \mathbf{0} \tag{2.1.9}$$

$$\nabla \cdot \mathbf{H}_M(\mathbf{x},t) = -\nabla \cdot \mathbf{M}(\mathbf{x},t) \tag{2.1.10}$$

Equations (2.1.7)-(2.1.10) allow to see the components $\mathbf{H}_J$ and $\mathbf{H}_M$ as produced only by the currents and only by the magnetization respectively. By summing equations (2.1.7) and (2.1.9) and equations (2.1.8) and (2.1.10) we see that the vector made of the sum of $\mathbf{H}_J$ and $\mathbf{H}_M$ satisfy both equations (2.1.6) and (2.1.4); therefore, from the unicity theorem, it follows that it coincides with the unknown magnetic field, i.e.

$$\mathbf{H}(\mathbf{x},t) = \mathbf{H}_J(\mathbf{x},t) + \mathbf{H}_M(\mathbf{x},t) \tag{2.1.11}$$

Equation (2.1.11) with the conditions (2.1.7)-(2.1.10) and (2.1.4) and (2.1.6) is usually referred to as the *Clebsh decomposition* of the magnetic field.

Since equation (2.1.8) states the solenoidality of the component $\mathbf{H}_J$ everywhere, the latter can be expressed as the curl of a vector magnetic potential $\mathbf{A}_J$, that is a regular vector function whose divergence can be arbitrarily assigned, as discussed in section

1.1. By introducing the vector magnetic potential in equation (2.1.7) and setting to zero its divergence, a vector Poisson equation is obtained and $\mathbf{A}_J$ can be expressed as

$$\mathbf{A}_J(\mathbf{x},t) = \frac{1}{4\pi}\int_{V_{NC}} \frac{\mathbf{J}^{ext}(\mathbf{x}',t)}{|\mathbf{x}-\mathbf{x}'|} d^3\mathbf{x}' \tag{2.1.12}$$

where V_{NC} represents the volume where the current density distribution has non-zero value. By taking the curl of equation (2.1.12) we obtain the following expression of $\mathbf{H}_J$, which is usually referred to as the Biot and Savart law.

$$\mathbf{H}_J(\mathbf{x},t) = \frac{1}{4\pi}\int_{V_{NC}} \frac{\mathbf{J}^{ext}(\mathbf{x}',t)\times(\mathbf{x}-\mathbf{x}')}{|\mathbf{x}-\mathbf{x}'|^3} d^3\mathbf{x}' \tag{2.1.13}$$

From equation (2.1.9) we see that the component $\mathbf{H}_M$ has zero curl everywhere, therefore it can be expressed as the gradient of a regular scalar function ψ named scalar magnetic potential, i.e.

$$\mathbf{H}_M(\mathbf{x},t) = -\nabla\psi(\mathbf{x},t) \tag{2.1.14}$$

By substituting equations (2.1.13) and (2.1.14) in equation (2.1.11) we express the magnetic field as

$$\mathbf{H}(\mathbf{x},t) = \frac{1}{4\pi}\int_{V_{NC}} \frac{\mathbf{J}^{ext}(\mathbf{x}',t)\times(\mathbf{x}-\mathbf{x}')}{|\mathbf{x}-\mathbf{x}'|^3} d^3\mathbf{x}' - \nabla\psi(\mathbf{x},t) \tag{2.1.15}$$

So far, in order to find an expression of the total magnetic field $\mathbf{H}$ at any point of the considered domain, we have decomposed it in two components $\mathbf{H}_J$ and $\mathbf{H}_M$ and we have obtained equation (2.1.15), where the magnetization $\mathbf{M}$ does not appear explicitly, rather it is "hidden" inside the scalar magnetic potential ψ. In fact by substituting equation (2.1.14) in equation (2.1.10) we obtain a scalar Poisson equation which allow us to relate the scalar potential to the magnetization **M** inside the superconducting region as follows

$$\psi(\mathbf{x},t) = \frac{1}{4\pi}\int_{V_{SC}} \frac{\nabla\cdot\mathbf{M}(\mathbf{x}',t)}{|\mathbf{x}-\mathbf{x}'|} d^3\mathbf{x}' \tag{2.1.16}$$

where V_{SC} represents the volume of the superconductor. If we are interested to relate the local magnetic flux density **B** to the magnetization inside the superconductor and the currents which circulate outside, we can substitute equations (2.1.16), (2.1.15) in the constitutive relation (1.2.1); however the resulting expression is not so easy to deal with numerically, for the magnetization **M** is subject to a second order differential operator. To accomplish the same task it possible to follow an alternative way. In fact, we recall that the magnetic flux density **B** is a soleinodal vector everywhere which can be expressed as the curl of a magnetic vector potential **A**; by introducing vector **A** with zero divergence inside the Ampere equation (2.1.4) and considering the constitutive relation (2.1.1) we obtain a Poisson equation which now has two source terms, one related to the magnetization of the superconductor and one to the currents outside, i.e.

$$\nabla^2\mathbf{A}(\mathbf{x},t) = -\mu_0\mathbf{J}^{ext}(\mathbf{x},t) - \mu_0\nabla\times\mathbf{M}(\mathbf{x},t) \tag{2.1.17}$$

By solving equation (2.1.16) we obtain [2,39] the following expression

$$\mathbf{A}(\mathbf{x},t) = \frac{\mu_0}{4\pi}\int_{V_{NC}} \frac{\mathbf{J}^{ext}(\mathbf{x}',t)}{|\mathbf{x}-\mathbf{x}'|} d^3\mathbf{x}' + \frac{\mu_0}{4\pi}\int_{V_{SC}} \frac{\mathbf{M}(\mathbf{x}',t)\times(\mathbf{x}-\mathbf{x}')}{|\mathbf{x}-\mathbf{x}'|^3} d^3\mathbf{x}' \tag{2.1.18}$$

By taking the curl of the vector magnetic potential defined above with respect to the coordinates of point **x**, it is possible, in principle, to calculate the magnetic flux density. As long as the field point **x** lies outside the volume V_{SC}, both the integrals on the left hand side of equation (2.1.18) are continuous as well as differentiable functions of **x** and the curl can be taken under the integral sign [39], i.e.

$$
\begin{aligned}
\mathbf{B}(\mathbf{x},t) = & -\frac{\mu_0}{4\pi}\int_{V_{NC}} \frac{\mathbf{J}^{ext}(\mathbf{x}',t)\times(\mathbf{x}-\mathbf{x}')}{|\mathbf{x}-\mathbf{x}'|^3} d^3\mathbf{x}' + \\
& -\frac{\mu_0}{4\pi}\int_{V_{SC}} \left(-\frac{\mathbf{M}(\mathbf{x}',t)}{|\mathbf{x}-\mathbf{x}'|^3} + \left(3\mathbf{M}(\mathbf{x}',t)\cdot\frac{(\mathbf{x}-\mathbf{x}')}{|\mathbf{x}-\mathbf{x}'|^5} \right)(\mathbf{x}-\mathbf{x}') \right) d^3\mathbf{x}'
\end{aligned}
\tag{2.1.19}
$$

Equation (2.1.19) corresponds to the calculation of the magnetic flux density as the sum of the elemental contributions arising from the infinitesimal currents and magnetizations located over V_{NC} and V_{SC} respectively; notwithstanding, if point **x** lies inside volume V_{SC} equation (2.1.19) does not any longer apply because the second integral becomes semi-convergent, i.e. its value, which is calculated as the limit of the integral over a volume obtained by excluding from V_{SC} a cavity surrounding the field point which shrinks to zero, changes with the change of the cavity shape from prolate to oblate with respect to the local direction of **M** [39]. However, both the integrals of equation (2.1.18) are always convergent, regardless if point **x** lies inside or outside volume V_{SC}, therefore is always possible to express the vector magnetic potential as a function of the sources. This property is very convenient if we are interested to relate the flux of the magnetic flux density **B** through any surface to the distribution of current and magnetization for it coincides with the loop integral of vector **A** over the border of the surface and can be calculated through equation (2.1.18).

Equations (2.1.5), (2.1.15) and (2.1.18), together with the characteristic of the superconducting material (2.1.3), form the basis of the model of the equivalent magnetic network which is developed in section 2.2.

2.2 The discretized problem and the equivalent magnetic network

Let us consider a system made of a superconducting region (SC) subject to the magnetic field produced by a current driven normal conducting coil (NC). The dimensions of the NC and SC domains and the frequency of variation of external magnetic field are such that the magnetoquasistatic approximation holds. In these conditions the superconductor reacts to the external magnetic field by expelling the field lines from inside. This effect can be taken in account by envisioning an induced distribution of magnetization arising in the superconductor which produces a magnetic field that cancels the external applied one from inside. As discussed in section 2.1, in this picture no currents are induced in the superconductor.

In order to determine the distribution of magnetization inside let us divide the superconducting region in a finite number N_E of three-dimensional elements. Let N_F be the number of faces of the discretization. N_{FB} of these faces lie on the boundary of the SC body while N_{FI} are inner faces ($N_F = N_{FI} + N_{FB}$). Let us also define a normal unit vector for all faces. We assume all the N_F fluxes of vector **B** through the faces of the discretized SC region and the N_E magnetic scalar potential in the centers of the elements as unknowns of the problem. This means that all the physical quantities involved in the calculation have to be expressed as a function of them. Moreover, we assume all the fluxes to be oriented according to the normal unit vector of the face, i. e. a positive flux is given by a magnetic flux density whose flux through the face, respect to the direction of the normal unit vector, is positive.

As an example let us refer to the system shown in figure 2.2.1, made of a superconducting cylinder placed in proximity of a normal conducting coil supplied by a current $I_{coil}(t)$. We assume a Cartesian coordinate system having the z axis parallel to axis of the cylinder and the origin coincident with its centre as reference system.

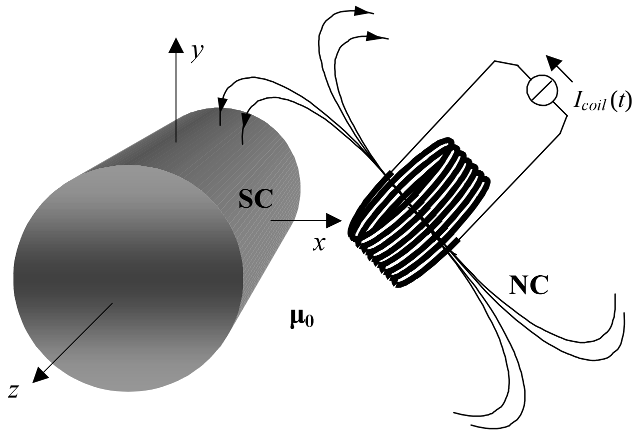

figure 2.2.1: superconducting cylinder subject to an external magnetic field

We subdivide the cylindrical volume in 6 prisms with triangular basis, as shown in figure 2.2.1. This very coarse mesh allows us to work out all the numerical details without being too cumbersome to deal with; the numerical procedure that we expose referring to it can be applied to more packed meshes or meshes made of elements with different shape (tetrahedron, parallelepipeds, prisms with different basis …).

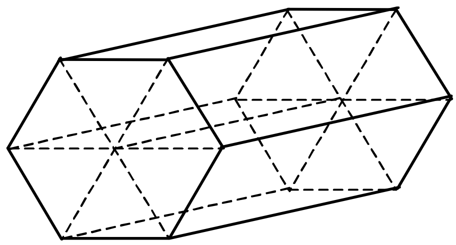

figure 2.2.2: mesh of the SC cylinder

The total number N_F of faces is equal to 24. The number N_{FB} of faces lying on the boundary of the SC cylinder is equal to 18 while the number N_{FI} of inner faces is equal to 6. Let us now associate an oriented graph $\mathcal{G}$ to the mesh of the superconducting domain in the following way

- any of the N_F faces of the mesh corresponds to a branch of the graph;
- any of the centers of the N_E elements of the SC mesh corresponds to a node of the graph; an additional node ∞ is provided in order to allow the

connection of the branches corresponding to a boundary face; the total number of nodes is equal to $N_E + 1$

- any branch is oriented according to normal unit vector of the corresponding face

The oriented graph relative to the mesh of figure 2.2.2, containing 7 nodes and 24 branches, is represented in figure 2.2.3.

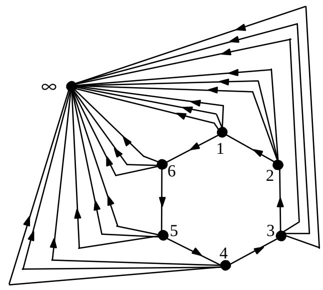

figure 2.2.3:orientedgraph associated to the 3D mesh of the SC cylinder

As it can be seen from the figure the additional node, which is indicated with ∞, collects all the branches associated to a boundary face; therefore the algebraic sum of the fluxes converging to it coincides with the total magnetic flux over the boundary of the superconducting region, which is zero being this a closed surface.

Let us start to express the mathematical equations which represent the physical constrains that the vectors of the unknown fluxes and potential must satisfy. Since the magnetic flux density **B** is a soleinodal vector at any point, its flux through any closed surface must be zero. According with this property, the algebraic sum of the magnetic fluxes through all the faces of any element must be equal to zero at any instant. By indicating with $\mathbf{\Phi}(t)$ the set of the N_F unknown fluxes at time t and using the incidence matrix $[\mathbf{A^{in}}]$ of the oriented graph $\mathcal{G}$ (see section 1.2, page 14, for the definition), having dimension $(N_E + 1) \times N_F$, we can express these equations a follow

$$[\mathbf{A^{in}}]\mathbf{\Phi}(t) = \mathbf{0} \tag{2.2.1}$$

Since any of equations (2.2.1) can be obtained by the sum of the others with opposite sign, one of them can be eliminated. We choose to eliminate the equation corresponding to node ∞. Moreover we assume arbitrarily one of the nodes of the graph but node ∞ as reference node; at this stage this only means that we omit from equations (2.2.1) the one relative to the row of matrix $[\mathbf{A}^{\mathbf{in}}]$ which refers to this node. It follows that the we obtain the following set of $(N_E - 1)$ independent equations which involves the N_F unknown fluxes

$$[\mathbf{A}]\boldsymbol{\Phi}(t) = \mathbf{0} \tag{2.2.2}$$

where matrix $[\mathbf{A}]$ is obtained from matrix $[\mathbf{A}^{\mathbf{in}}]$ by removing the rows corresponding to node ∞ and to the reference node. We stress that the latter omitted equation is not dependent from the others.

Let us now consider equation (2.1.15), which relates the total magnetic field at any point of the superconductor, to the currents of the normal conducting region and the magnetic scalar potential. By taking the line integral of the magnetic field over a path connecting whatever couple of points $\mathbf{x}_h$ and $\mathbf{x}_k$ belonging to the SC domain and oriented from $\mathbf{x}_h$ to $\mathbf{x}_k$ the following equation is obtained:

$$\int_{\mathbf{x}_h}^{\mathbf{x}_k} \mathbf{H}(\mathbf{x},t)\cdot d\mathbf{x} = \psi(\mathbf{x}_h,t) - \psi(\mathbf{x}_k,t) + \int_{\mathbf{x}_h}^{\mathbf{x}_k} \left(\frac{1}{4\pi} \int_{V_{NC}} \frac{\mathbf{J}^{ext}(\mathbf{x}',t)\times(\mathbf{x}-\mathbf{x}')}{\left|\mathbf{x}-\mathbf{x}'\right|^3} d^3\mathbf{x}' \right)\cdot d\mathbf{x} \tag{2.2.3}$$

All the terms of equation (2.2.3) have the dimension of a magneto-motive force. By considering the mesh of the superconducting domain, it is possible to associate at any face that does not lie on the boundary an equation of the same type of (2.2.3). In fact, to any of the N_{FI} inner faces it corresponds an integration path made of the union of the segments connecting the centre of the face to the centers of the elements which share it; this integration path is oriented according to the normal unit vector of the face.

By substituting the constitutive relation of the material (2.1.1) inside equation (2.2.3) and considering that the magnetization depends on the magnetic flux density through the non linear and hysteretic relation (2.1.3), we obtain

$$\int_{\mathbf{x}_h}^{\mathbf{x}_k} \frac{\mathbf{B}(\mathbf{x},t)}{\mu_0} \cdot d\mathbf{x} - \int_{\mathbf{x}_h}^{\mathbf{x}_k} \mathcal{M}_B(\mathbf{B}(\mathbf{x},\tau), \tau \le t) \cdot d\mathbf{x} =$$
$$\psi(\mathbf{x}_h,t) - \psi(\mathbf{x}_k,t) + \int_{\mathbf{x}_h}^{\mathbf{x}_k} \left(\frac{1}{4\pi} \int_{V_{NC}} \frac{\mathbf{J}^{ext}(\mathbf{x}',t) \times (\mathbf{x}-\mathbf{x}')}{|\mathbf{x}-\mathbf{x}'|^3} d^3\mathbf{x}' \right) \cdot d\mathbf{x} \tag{2.2.4}$$

Actually, the non linear and hysteretic relation that link the vectors **M** and **B** depends also on the temperature; in the following we will assume the superconducting region to be in thermal equilibrium with assigned temperature, thus neglecting the effects of the local heating. For the cases where the thermal effects become important, the present electromagnetic model must be coupled with a thermal model which allow to calculate at any time, the temperature distribution inside the SC domain.

Since the unknowns of the discretized problem are the fluxes through the faces and the potentials in the centers of the elements, we have to express all the physical quantities involved in equation (2.2.4) as a function of them. To accomplish this task we assume the magnetic flux density **B** to be an uniform vector inside any element of the SC domain. Its value can be related to the fluxes through the faces of the discretization by following the same procedure used in the model of the equivalent electric network to relate the uniform current density **J** to the currents through the faces (see section 1.2, pages 18-20); i.e. the magnetic flux density **B** at any point of the superconducting domain can be expressed, at any instant *t*, as follow

$$\mathbf{B}(\mathbf{x},t) = [\mathbf{K}(\mathbf{x})]\mathbf{\Phi}(t) \tag{2.2.5}$$

Matrix **[K(x)]**, having dimension $3 \times N_F$, is an element-wise uniform matrix, i. e. its elements are the same for all points **x** belonging to the same geometric element of discretized region SC. To determine its value at a given point $\mathbf{x}'$ is only necessary to find out the element *i* of the mesh to which point $\mathbf{x}'$ belong to and then to calculate it as reported in equation (1.2.14). Matrix **[K(x)]** is very sparse; in fact only columns which are relative to currents flowing through the faces of the element containing point **x** are non zero. This means that the reconstruction of magnetic flux density at any point is strictly local, i. e. it is only contributed by fluxes in the vicinity of the point. In principle is possible to apply a linear (or even higher order) reconstruction of the magnetic flux density from the fluxes, by following the procedure described in section 1.7 for the current density; however in this case the number or unknown fluxes and the complexity of the numerical problem increase very much.

For what concern the current of the normal conducting coil we assume that it distributes uniformly inside any turn. With these assumptions the current density $\mathbf{J}^{\text{ext}}$ at any point $\mathbf{x}$ of normal conducting region is a known quantity at any instant t and can be expressed as

$$\mathbf{J}^{ext}(\mathbf{x},t) = \mathbf{k}_{NC}(\mathbf{x}) I_{coil}(t) \tag{2.2.6}$$

where $\mathbf{k}_{NC}(\mathbf{x})$ is the vector given by the ratio between the unit vector tangent to the direction of the turn at point $\mathbf{x}$ and the area of its cross section.

By substituting equations (2.2.5) and (2.2.6) in equation (2.2.4) the following relation is obtained

$$\begin{aligned} &\left(\int_{\mathbf{x}_h}^{\mathbf{x}_k} \frac{d\mathbf{x}^T \left[\mathbf{K}(\mathbf{x})\right]}{\mu_0} \right) \mathbf{\Phi}(t) - \int_{\mathbf{x}_h}^{\mathbf{x}_k} d\mathbf{x}^T \mathcal{M}_B\left(\left[\mathbf{K}(\mathbf{x})\right] \mathbf{\Phi}(\tau), \tau \le t \right) = \\ &\qquad \psi(\mathbf{x}_h, t) - \psi(\mathbf{x}_k, t) + I_{coil}(t) \int_{\mathbf{x}_h}^{\mathbf{x}_k} d\mathbf{x}^T \left(\frac{1}{4\pi} \int_{V_{NC}} \frac{\mathbf{k}_{NC}(\mathbf{x}') \times (\mathbf{x} - \mathbf{x}')}{\left|\mathbf{x} - \mathbf{x}'\right|^3} d^3\mathbf{x}' \right) \end{aligned} \tag{2.2.7}$$

This equation states a non linear link between the fluxes of the SC region, the potentials of the nodes of the SC mesh, and the current circulating through the external coil. The link is hysteretic, i.e. it depends on the sequence of the values that the vector of the unknown fluxes has assumed from the initial to the current instant. The line integral from $\mathbf{x}_h$ to $\mathbf{x}_k$ can be split in the sum of the integrals from $\mathbf{x}_h$ to the centre of the face shared by the two elements and from the latter to $\mathbf{x}_k$. Since matrix $[\mathbf{K}(\mathbf{x})]$ is element wise uniform, the integrating function $\mathcal{M}_B$ can be moved out and the second integral of the left side can be expressed as the product of a non linear function of the fluxes with a vector of geometrical coefficients. However, if the considered material is not homogeneous, the constitutive relation depends explicitly on the point and this manipulation cannot be applied.

Let us denote with i the unique face of the SC mesh associated to points $\mathbf{x}_h$ and $\mathbf{x}_k$ and with $\Phi_i(t)$ the magnetic flux through it. The right side of equation (2.2.7) contains the difference of the magnetic scalar potentials at the points $\mathbf{x}_h$ and $\mathbf{x}_k$, and an impressed magneto-motive term, that we indicate with $m^{ext}{}_i(t)$, given by the product of a dimensionless geometrical coefficient n_i^{coil}, and the current flowing through the coil. The term represented by the first left hand integral is a linear function of all fluxes. Let us indicate with $m^0{}_i(t)$ this quantity and with $\boldsymbol{r}_i$ the vector of the geometric coefficients of the linear relation, which have the dimension of a magnetic reluctance, that is H^{-1}. Finally, the second term of the right side is given by a non linear and hysteretic function of these fluxes. We denote with $m^m{}_i(t)$ this term and with $\gamma_i^i(\boldsymbol{\Phi}(\tau), \tau \le t)$ the relative function. The top script i of function γ denotes that it is associated to an inner face. Indeed, since the reconstruction of the magnetic flux density ($[\mathbf{K}(\mathbf{x})]\boldsymbol{\Phi}(t)$) is strictly local and the integrals are calculated over the segment connecting the points $\mathbf{x}_h$ and $\mathbf{x}_k$, both the two latter terms depend only on the magnetic fluxes through the faces of the elements which are crossed by the integration path.

Likewise the case of equation (1.2.18) (see section 1.2, page 22), the above inspection of the various terms allows us to see equation (2.2.7) a the instantaneous balance of the magneto-motive forces relative to a magnetic circuit branch derived from two nodes h and k with potential $\psi(\mathbf{x}_h,t)$ and $\psi(\mathbf{x}_k,t)$ respectively and containing an impressed magneto-motive force generator $m^{ext}{}_i(t)$, a linear flux-controlled magneto-motive force generator $m^0{}_i(t)$ and a non linear flux-controlled magneto-motive force generator $m^M{}_i(t)$ related to the magnetization. A picture of this circuit branch is shown in figure 2.2.4.

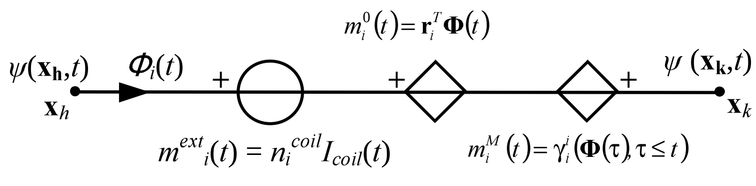

figure 2.2.4:circuit scheme of equation (2.2.7)

By using the symbols introduced above, equation (2.2.7) can be rewritten as

$$\psi(\mathbf{x}_h,t)-\psi(\mathbf{x}_k,t)-n_i^{coil}I_{coil}(t)=\mathbf{r}_i^T\mathbf{\Phi}(t)-\gamma_i^i(\mathbf{\Phi}(\tau),\tau\leq t) \tag{2.2.8}$$

where T denotes the transpose operator.

In order to get a physical understanding of equation (2.2.7) and its circuit interpretation (2.2.8) we consider a set of integration paths, inside the SC domain, which form a closed loop. By assigning a circulation direction and summing or subtracting the equations (2.2.7) relative to every segment of the loop depending on whether the corresponding segment is or is not oriented according to the circulation direction, the potentials of the nodes elides and the resulting relation coincides with the Ampere law applied to the loop line. This relation is expressed in a Hopkinson-like form because all the field quantities involved are given as a function of the magnetic fluxes through the faces of the discretization. Let us agree to refer for a moment to a linear magnetic material having magnetic susceptibility χ; since in this case the magnetization is proportional to the magnetic field through the non-dimensional coefficient χ, the equation of balance of the magneto-motive forces acting on the loop can be expressed as

$$I_{coil}(t)\sum_{\substack{i\\loop}}\pm n_i^{coil}=\sum_{\substack{i\\loop}}\pm\mathbf{r}_i^T\mathbf{\Phi}(t)-\sum_{\substack{i\\loop}}\pm\mathbf{r}_{M\,i}^{\;T}\mathbf{\Phi}(t) \tag{2.2.9}$$

where the sums involves all the segments forming the loop and vector $\mathbf{r}_{M\,i}^{\;T}$ is defined as:

$$\mathbf{r}_{M\,i}^{\;T}=\int_{\mathbf{x}_h}^{\mathbf{x}_k}d\mathbf{x}^T\,\frac{\chi[\mathbf{K}(\mathbf{x})]}{\mu_0(\chi+1)} \tag{2.2.10}$$

The term on the left side of equation (2.2.9) represents the total magneto-motive force acting on the loop, which coincides with the total current linked. If the coil was placed in the empty space, the total magneto-motive force would be balanced only by the first term of the right hand side, as the second term would be zero. Therefore, the further term on the right represents the contribution of the material. In the case of diamagnetic behavior, i.e. $\chi < 0$, the norm of the resulting vector $\sum_{i \atop loop} \pm \mathbf{r}_i^T - \sum_{i \atop loop} \pm \mathbf{r}_{M\,i}^{\,T}$, which multiply the set of the fluxes inside the material, is greater than the norm of vector $\sum_{i \atop loop} \pm \mathbf{r}_i^T$ which multiply the fluxes produced by the same current in the empty space, and the resulting magnetic flux density is weaker, as expected. If the material approaches the perfect diamagnetism, i.e. $\chi \to -1$, the norm of the resulting vector increases without bound thus to provide the condition of zero flux everywhere inside.

We have seen before that it is possible to associate at every of the N_{FI} faces which do not lie on the boundary of the domain an equation of the type of (2.2.8). By recalling the oriented graph $\mathcal{G}$ associated to the mesh, we can state the same property by saying that an equation of the same type of (2.2.8) can be associated to each branch that does not converge to node ∞. The unknown of these equations are the N_E magnetic scalar potentials in the centers of the elements and the N_F fluxes through the faces. In stating the conditions of zero algebraic sum for the fluxes through all the faces of every element of the mesh (equation 2.2.2) we left one element out and we identified the node of the graph corresponding to its centre as reference node. Since we are not interested in determining the absolute values of the potentials (all the field quantities are related to the scalar potential through differential operators), we can assign value zero to the magnetic scalar potential of the reference node and express the set of the N_{FI} independent equations of the type of (2.2.8) in the following concise form

$$[\mathbf{A}_{\mathbf{RED}}]^T \mathbf{\Psi}(t) - \mathbf{N}\, I_{coil}(t) = [\mathbf{R}]\mathbf{\Phi}(t) + \mathbf{\Gamma}_I\left(\mathbf{\Phi}(\tau), \tau \le t\right) \qquad (2.2.11)$$

where the elements of vector $\mathbf{\Psi}(t)$ now represent the difference among the potentials of the $(N_E - 1)$ “free” nodes and the potential of the reference node. Matrix $[\mathbf{A}_{\mathbf{RED}}]$, having dimension $N_{FI} \times (N_E - 1)$, is obtained from matrix $[\mathbf{A}]$ of equation (2.2.2) by eliminating the columns referring to the fluxes associated to the boundary faces, $\mathbf{N}$ is the vector of the N_{FI} coefficients n_i^{coil} which multiply the current of the external coil, **[R]** is the $N_{FI} \times N_F$ matrix of reluctances obtained by staking vectors $\mathbf{r}_i^T$ of all equations (2.2.8) and $\mathbf{\Gamma}_I(\mathbf{\Phi}(\tau), \tau \le t)$ is the vector of the N_{FI} scalar function $\gamma_i^i(\mathbf{\Phi}(\tau), \tau \le t)$.

It is worth to notice that, in developing the model of the equivalent electric network for the calculation of the current distribution induced inside a superconducting bulk by the change with time of an external magnetic field, we followed a route completely analogous to the one followed so far in this section; i.e. we stated as many independent constrains of zero algebraic sum for the currents as the number of the elements less one (equation (1.2.2)), and, through the integration of the electric field, as many links between the currents and the potentials as the number of the inner faces (equation (1.2.23)). In the present section we have done the same, except replacing vector **J** with **B** and vector **E** with **H**, and we have obtained equations (2.2.2) and (2.2.11). However, despite the fact that the set of equations (1.2.2) and (1.2.23) was sufficient to solve the electric problem (for they were as many as the unknowns there introduced), equations (2.2.2) and (2.2.11) are not sufficient to solve the magnetic one. In fact, these equations form a set of ($N_{FI} + N_E - 1$) scalar equations whereas the unknowns are N_F fluxes and ($N_E - 1$) potentials, therefore N_{FB} equations are missing. This substantial mathematical difference among the electric and the magnetic problem arises from the fact that in the former case the boundary conditions are specified as zero normal component of the current density all over the border of the domain. In terms of equivalent circuit quantities this implies that the currents flowing through the N_{FB} faces lying on the border are all zero and do not need to be introduced as unknowns. In the latter case the condition of zero normal component of the magnetic flux density over the border does not hold, therefore a further set of N_{FB} fluxes must be to be introduced and as many equations must be stated.

In order to specify the boundary conditions, we can refer to equation (2.1.18), relating the vector magnetic potential to the sources. According to the stokes theorem the magnetic flux through a generic surface can be expressed by means of the loop integral of the vector magnetic potential over the border of the face; in particular, the magnetic flux $\Phi_j(t)$ at time t through the generic face j lying on the boundary of the superconductor can be expressed as

$$\Phi_j(t) = \oint_{\partial\Sigma_j} \left(\frac{\mu_0}{4\pi} \int_{V_{NC}} \frac{\mathbf{J}^{ext}(\mathbf{x}',t)}{\left|\mathbf{x}-\mathbf{x}'\right|} d^3\mathbf{x}' \right) \cdot d\mathbf{x} + \\ + \oint_{\partial\Sigma_j} \left(\frac{\mu_0}{4\pi} \int_{V_{SC}} \frac{\mathbf{M}(\mathbf{x}',t) \times (\mathbf{x}-\mathbf{x}')}{\left|\mathbf{x}-\mathbf{x}'\right|^3} d^3\mathbf{x}' \right) \cdot d\mathbf{x} \tag{2.2.12}$$

where $\partial\Sigma_j$ represents the border line of face *j*. By substituting the constitutive relation of the material (2.1.1) and equations (2.2.5) and (2.2.6) in equation (2.2.12) the following relation is obtained

$$\Phi_j(t) = I_{coil}(t) \oint_{\partial\Sigma_j} d\mathbf{x}^T \left(\frac{\mu_0}{4\pi} \int_{V_{NC}} \frac{\mathbf{k}_{NC}(\mathbf{x}')}{\left|\mathbf{x}-\mathbf{x}'\right|} d^3\mathbf{x}' \right) + \\ + \oint_{\partial\Sigma_j} d\mathbf{x}^T \left(\frac{\mu_0}{4\pi} \int_{V_{SC}} \frac{\mathcal{M}_B\left(\left[\mathbf{K}(\mathbf{x}')\right]\boldsymbol{\Phi}(\tau), \tau \le t\right) \times (\mathbf{x}-\mathbf{x}')}{\left|\mathbf{x}-\mathbf{x}'\right|^3} d^3\mathbf{x}' \right) \tag{2.2.13}$$

The above equation allows to see the flux through face *j* lying on the boundary as composed by two contributes: a firs contribute $\Phi_j^{coil}(t)$, proportional to the current of the normal coil through a coefficient l_j^{coil} having the dimension of an inductance and a second contribute $\Phi_j^{m}(t)$ due to the magnetization of the superconductor, which is expressed by a non linear and hysteretic function of all fluxes $\gamma_j^b(\boldsymbol{\Phi}(\tau), \tau \le t)$, i. e.

$$\Phi_j(t) = l_j^{coil} I_{coil}(t) + \lambda_j^b(\boldsymbol{\Phi}(\tau), \tau \le t) \tag{2.2.14}$$

The top script *b* of function γ denotes that it is associated to a boundary face. Maintaining the circuit view of the problem we can see the flux through the boundary face *j*, to whom correspond a branch of the graph which converges to node ∞, as produced by an independent and a controlled flux generator, as shown in figure 2.2.5.

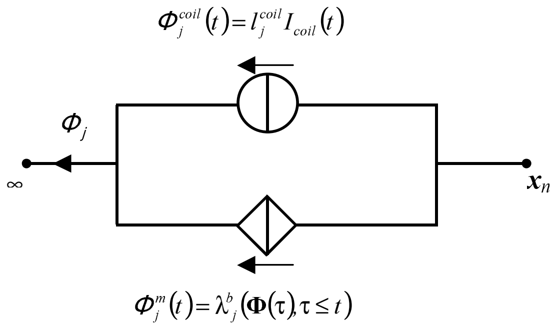

figure 2.2.5:circuit scheme of equation (2.2.14)

The node $\boldsymbol{x}_n$ coincides with the center of the element to which the boundary face j belongs to, while the node ∞, which was yet introduced in the graph associated to the mesh of the superconductor (see figure 2.2.3), represents the far surface (placed at infinity) where all the lines of the magnetic flux density shut up. The infinity node ∞ is shared by all the couples of generators associated to every boundary face; with this assumption the algebraic sum of the fluxes converging to it coincides with the total magnetic flux over the boundary of the superconducting domain. In order not to violate the physics of the problem and the consistency of its circuit picture we have to be sure that this flux is equal to zero. However, since from the incidence equations, beside the one relative to the infinite node, we eliminated a further one of them referring to the node assumed as reference, this condition is not any longer automatically satisfied. Notwithstanding, we can overcome the impasse by considering that the loop integral of the vector potential in equation (2.2.13) relative to a generic boundary face is calculated as the sum of the line integrals over the segments which form its border. Whatever boundary segment is shared by two faces and, if both are oriented inward or outward, its contribution to the two fluxes has equal magnitude and opposite sign. Therefore the condition of zero algebraic sum of the fluxes through the boundary is indirectly maintained through equation (2.2.13)

The set of the N_{FB} independent equations of the type of the (2.2.14), which express the fluxes through the boundary faces as a function of all the fluxes and the current of the normal coil, can be written in the following way

$$[\mathbf{S}]\mathbf{\Phi}(t) = \mathbf{L}\, I_{coil}(t) + \mathbf{\Gamma}_B(\mathbf{\Phi}(\tau), \tau \le t) \qquad (2.2.15)$$

where **[S]** is a matrix having dimension $N_{FB} \times N_F$, whose generic element s_{ij} is equal to 1 if the *j-th* flux of vector $\mathbf{\Phi}(t)$ flows through the *i-th* boundary face and is equal to 0 otherwise, **L** is the vector of the N_{FB} coefficients l_j^{coil} which multiply the current of the external coil in equation (2.2.14) and $\mathbf{\Gamma}_B(\mathbf{\Phi}(\tau), \tau \le t)$ is the vector of the N_{FB} scalar function $\lambda_j^b(\mathbf{\Phi}(\tau), \tau \le t)$.

From equations (2.2.2), (2.2.11) and (2.2.15) it follows that the entire superconducting domain can be schematized by means of an equivalent magnetic network, having N_F branches and ($N_E + 1$) nodes. The circuit unknowns are N_F fluxes through the faces and ($N_E - 1$) potentials in the nodes (recall the potential of the reference node is arbitrarily assumed to be equal to zero and the potential of node ∞ cannot be determined). The solving system of the equivalent magnetic network, that is a set of ($N_F + N_E - 1$) equations in the ($N_F + N_E - 1$) unknowns can be written as

$$\begin{cases} [\mathbf{A}]\mathbf{\Phi}(t) = \mathbf{0} \\ [\mathbf{A}_{\mathbf{RED}}]^T \mathbf{\Psi}(t) - \mathbf{N}\, I_{coil}(t) = [\mathbf{R}]\mathbf{\Phi}(t) + \mathbf{\Gamma}_I(\mathbf{\Phi}(\tau), \tau \le t) \\ [\mathbf{S}]\mathbf{\Phi}(t) = \mathbf{L}\, I_{coil}(t) + \mathbf{\Gamma}_B(\mathbf{\Phi}(\tau), \tau \le t) \end{cases} \qquad (2.2.16)$$

System (2.2.24) can be solved directly to obtain the time evolution of the potentials and fluxes through the faces of the discretized the SC region; once the vector $\mathbf{\Phi}(t)$of all fluxes at time t has been calculated, the instantaneous distribution of magnetic flux density and magnetization can be reconstructed by means of equation (2.2.5) and (2.1.3) respectively. However, likewise the case of the model of the equivalent electric network, also in this case it is possible to apply the tree-cotree decomposition of the graph presented in section 1.3, in order to obtain a solving system having a reduced size. In fact, by means of algebraic manipulations on matrix **[A]** of system (2.2.16) (see section 1.3, page 30), it is possible select a tree of the graph associated to the magnetic network and express the vector $\mathbf{\Phi}_{\mathbf{T}}(t)$ of the ($N_E - 1$) fluxes of the tree branches as a function of the vector $\mathbf{\Phi_C}(t)$ of the (N_F – N_E + 1) fluxes of the cotree branches as follow

$$\mathbf{\Phi_T}(t) = -[\mathbf{C}]\mathbf{\Phi_C}(t) \tag{2.2.17}$$

where matrix **[C]**, having dimension (N_E – 1) × (N_F – N_E + 1),coincides with the matrix of the fundamental cuts associated to the tree resulting from the decomposition algorithm. Moreover, the second of matrix equations (2.2.16) can be expressed as

$$[\mathbf{A_{RED}}]^T\,\mathbf{\Psi}(t) - [\mathbf{Id}]\mathbf{N}I_{coil}(t) = [\mathbf{Id}][\mathbf{R}]\mathbf{\Phi}(t) + [\mathbf{Id}]\mathbf{\Gamma}_I(\mathbf{\Phi}(\tau), \tau \le t) \tag{2.2.18}$$

where **[Id]** represents the N_{FI} × N_{FI} identity matrix. By applying to matrix $[\mathbf{A_{RED}}]^T$ some algebraic manipulations (see section 1.3, page 33) we obtain

$$\begin{aligned}&\begin{pmatrix}[\mathbf{Id}]_{N_E-1}\\ [\mathbf{0}]\end{pmatrix}\mathbf{\Psi}(t) - [\mathbf{Id}]'\,\mathbf{N}\,I_{coil}(t) = \\ &\qquad [\mathbf{Id}]'\begin{pmatrix}[\mathbf{R}]_{11} & [\mathbf{R}]_{12}\\ [\mathbf{R}]_{21} & [\mathbf{R}]_{22}\end{pmatrix}\begin{pmatrix}\mathbf{\Phi_T}(t)\\ \mathbf{\Phi}_C(t)\end{pmatrix} + [\mathbf{Id}]'\,\mathbf{\Gamma}_I(\mathbf{\Phi_T}(\tau), \mathbf{\Phi_C}(\tau), \tau \le t)\end{aligned} \tag{2.2.19}$$

where $[\mathbf{Id}]_{N_E-1}$ represents the (N_E – 1) × (N_E – 1) identity matrix, **[0]** is an (N_{FI} – N_E + 1) matrix made of all zeros and matrix $[\mathbf{Id}]'$ represents the modified matrix **[Id]**[1]. Matrixes $[\mathbf{R}]_{11}$ and $[\mathbf{R}]_{12}$ are minors having both (N_E – 1) rows and (N_E – 1) and (N_{FI} – N_E + 1) columns respectively, whereas the number of rows of minors $[\mathbf{R}]_{21}$ and $[\mathbf{R}]_{22}$ is equal to (N_{FI} – N_E + 1). By substituting equation (2.2.17) in equation (2.2.19) and considering only the last (N_{FI} – N_E + 1) rows, the following relation obtained

$$[\mathbf{Id}]''\,\mathbf{N}\,I_{coil}(t) = \left([\mathbf{Id}]''\,[\mathbf{R}]_{22} - [\mathbf{Id}]''\,[\mathbf{R}]_{21}[\mathbf{C}]\right)\mathbf{\Phi}_C(t) + [\mathbf{Id}]''\,\mathbf{\Gamma}_I{}'(\mathbf{\Phi_C}(\tau), \tau \le t) \tag{2.2.20}$$

[1] The number of inner faces is always greater or equal to the number of elements less one. If the equality holds equations, i.e. if it is not possible to form a closed loop by combining branches referring to inner faces only, (2.2.2) and (2.2.15) form yet a set of N_F relations involving only the fluxes which can be solved directly without considering equations (2.2.11). The latter can be used after the flux are determined if the magnetic scalar potentials are required.

where matrix $\mathbf{[Id]}''$ is made of the last ($N_{FI} - N_E + 1$) rows of matrix $\mathbf{[Id]}'$ and $\mathbf{\Gamma}_I{}'$ is a non linear and hysteretic vector function with ($N_{FI} - N_E + 1$) components depending only on the cotree fluxes. These equations, which do not involve the potentials, are indeed the magneto-motive forces balance equations of all the independent loops made of branches referring to inner faces. Finally, by rearranging the columns of matrix **[S]** by placing first those referring to the tree fluxes and later those referring the cotree ones, the third of matrix equations (2.2.16) can be expressed as

$$[\mathbf{S}_T]\mathbf{\Phi}_T(t) + [\mathbf{S}_C]\mathbf{\Phi}_C(t) = \mathbf{L}\, I_{coil}(t) + \mathbf{\Gamma}_B(\mathbf{\Phi}(\tau), \tau \le t) \tag{2.2.21}$$

where matrixes $[\mathbf{S}_T]$ and $[\mathbf{S}_C]$ have ($N_E - 1$) and ($N_F - N_E + 1$) columns respectively. By substituting equation (2.2.17) in equation (2.2.21) and considering equation (2.2.20) as well, the following system is obtained

$$[\mathcal{P}]\mathbf{\Phi}_C(t) + \mathcal{F}(\mathbf{\Phi_C}(\tau), \tau \le t) = \mathcal{q}\, I_{coil}(t) \tag{2.2.22}$$

where matrix $[\mathcal{P}]$, function $\mathcal{F}$ and vector $\mathcal{q}$ are defined as follow

$$[\mathcal{P}] = \begin{pmatrix} \mathbf{[Id]}''[\mathbf{R}]_{22} - \mathbf{[Id]}''[\mathbf{R}]_{21}\mathbf{[C]} \\ [\mathbf{S}_C] - [\mathbf{S}_T]\mathbf{[C]} \end{pmatrix} \tag{2.2.23}$$

$$\mathcal{F}(\mathbf{\Phi_C}(\tau), \tau \le t) = \begin{pmatrix} \mathbf{[Id]}''\,\mathbf{\Gamma}_I{}'(\mathbf{\Phi_C}(\tau), \tau \le t) \\ -\mathbf{\Gamma}_B{}'(\mathbf{\Phi_C}(\tau), \tau \le t) \end{pmatrix} \tag{2.2.24}$$

and

$$\mathcal{q} = \begin{pmatrix} \mathbf{[I]}''\,\mathbf{N} \\ \mathbf{L} \end{pmatrix} \tag{2.2.25}$$

$\mathbf{\Gamma}_B{}'$ of equation (2.2.24) is a non linear and hysteretic vector function with (N_{FB}) components depending only on the cotree fluxes.

System (2.2.22) consists of ($N_F - N_E + 1$) equations containing only the ($N_F - N_E + 1$) fluxes of the cotree branches as unknowns, and allows to calculate numerically their time evolution. Due to the reduced number of unknowns, the calculation time and the CPU requirements are less onerous than those of the full solving system (2.2.16). The missing (N_E – 1) fluxes of the tree branches and, if required, the magnetic scalar potentials of the nodes, can be determined at a later time by means of equations (2.2.17) and (2.2.19). The magnetic flux density and magnetization distributions inside the SC region can be calculated, instant by instant, through equations (2.2.5) and (2.1.3) respectively. The definition of the hysteretic relation (2.1.3) is the topic of the next section.

The non-linear system (2.2.22) requires a fast and reliable numerical technique to be efficiently solved. In dealing with magnetic hysteresis problems, several efficient hysteresis engines have been so far proposed [40,41]; however when coupled with a numerical technique for solving non-linear equations, strong convergence problem have been observed [42,43]. In order to solve system (2.2.22) it is possible to use a fixed point technique [44] by rewriting it in the following way

$$\mathbf{\Phi}_C(t) = \mathcal{G}\left(\left(\mathbf{\Phi_C}(\tau), \tau \le t\right), I_{ext}(t)\right) \tag{2.2.26}$$

where

$$\mathcal{G}\left(\left(\mathbf{\Phi_C}(\tau), \tau \le t\right), I_{ext}(t)\right) = -[\mathcal{P}]^{-1}\,\mathcal{F}\left(\mathbf{\Phi_C}(\tau), \tau \le t\right) + [\mathcal{P}]^{-1}\,\mathcal{q}\, I_{ext}(t) \tag{2.2.27}$$

By considering a given instant t and assigning to it an attempt solution $\mathbf{\Phi}_C{}^0(t)$, the vector $\mathbf{\Phi}_C(t)$ of the unknowns can be determined through the following iterative process

$$\mathbf{\Phi}_C{}^n(t) = \mathcal{G}\left(\left(\mathbf{\Phi}_C{}^{n-1}(\tau), \tau \le t\right), I_{ext}(t)\right) \tag{2.2.28}$$

In order to assure the convergence of the above sequence to the fixed point of function $\mathscr{G}$ this must be contractive [44]. This condition can be assured by replacing the non-linear hysteretic relation (2.1.3) between magnetization **M** and magnetic flux density **B** is with the sum of a linear term $\nu\mathbf{B}$ and an residual term $\mathbf{M}_{mod}$ defined as follow [45-48]:

$$\mathbf{M}_{mod}(\mathbf{x},t) = \mathcal{M}_B(\mathbf{B}(\mathbf{x},\tau), \tau \leq t) - \nu\mathbf{B}(\mathbf{x},\tau) \tag{2.2.29}$$

Equation (2.2.29) implies that, by a suitable choice of the conventional permeability ν, the contracting mapping principle applies to function $\mathscr{G}$ and the fixed point algorithm converges, whatever is the attempt solution $\mathbf{\Phi}_C{}^0(t)$ chosen, without posing any constraint on the smoothness of the magnetization characteristic. Of course, the modified material characteristics leads to adjunctive linear terms in equations (2.2.11) and (2.2.15). However, since the factor ν is constant, these terms don't change during the iterative process and can be calculated once for all at the beginning and incorporated in matrix $[\mathbf{R}]$ and $[\mathbf{S}]$ respectively.

In ending this section we point out that, even if in the model of the equivalent magnetic network equation (2.2.12), which does not involve the magnetic scalar potential, is used only for the boundary faces, it could be stated also for any inner face of the discretization. Therefore, by stating it for all the N_F faces of the mesh, and considering that, as discussed above, it implicitly respects the incidence equations (2.2.2), it is possible to obtain a solving system, made of N_F equations of the form of (2.2.14), which contains only the set of the N_F fluxes as unknowns. This system can be further reduced by means of the tree-cotree decomposition algorithm. By solving the reduced system the time evolution of the magnetic flux density and magnetization inside the superconducting region can be reconstructed. Even though very attractive for it does not introduce at all the magnetic scalar potential, this alternative approach is problematic for what concern the convergence aspects. In fact, it has been observed that, for a wide class of problems, by using system (2.2.22) the numerical convergence is reached yet through very coarse meshes, whereas, by using the alternative approach, a very packed discretization is needed. In order to understand the reasons of this different behavior let us refer, for simplicity, to a linear magnetic material and consider the two magnetic configurations shown in figure 2.2.7. To calculate the magnetic flux density distribution inside magnetizable regions, after the discretization is introduced, we define the full equivalent magnetic network and then apply the tree-cotree decomposition to obtain the reduced system 2.2.22 which does not contains the magnetic scalar potentials.

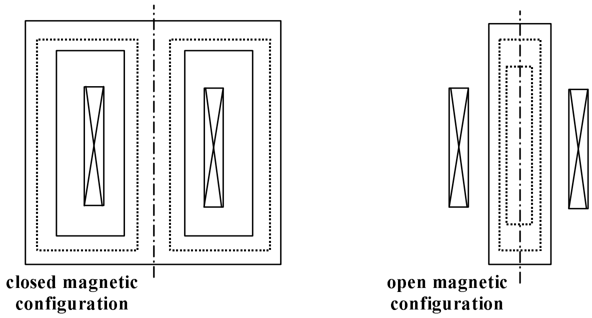

figure 2.2.7:magnetic configurations

When a closed magnetic core is considered, whatever the chosen mesh, at least two of the equations of the reduced system states the balance of the magneto-motive force along a line which link the coil. In case of high magnetic susceptibility these equations allow to determine the dominant component of the magnetic flux density inside the core. The leakage fluxes are taken in account by means of the equations referring to the boundary face. The more they are negligible the more these latter equations are unessential and the convergence is reached with not refined meshes. By following the alternative approach the equations of balance of the magneto-motive forces are not exploited and no dominant components are found; all the fluxes are then equivalent and an accurate distribution can be reached only by means of refine meshes.

Contrariwise, by considering the case of open core, whatever the chosen mesh, there are no loops that link the coil. Therefore the equations of balance of the magneto-motive forces are exploited but they are not relevant and the two approaches are equivalent in terms of numerical convergence.

It is worth to notice that if a small air gap exists in a closed core configuration, it is convenient to include it in the discretization by assigning to the corresponding elements a zero magnetic susceptibility, thus to recover the possibility of using some magneto-motive forces equations and speed up the convergence.

2.3 The hysteresis model

In section 2.1 we have seen as, with respect to its magnetic behavior, a superconductor can be schematized as a magnetizable material having null electric conductivity. In this picture no currents circulate inside when the superconductor is subject to an external magnetic field and a magnetization distribution is induced to take account of the diamagnetic behavior. The local dependence of the induced magnetization on the magnetic flux density is given by the experimental observed hysteresis loops, which play the role of constitutive relation of the superconducting material [17,18]. The same approach is used to calculate the magnetic flux distribution in ferromagnetic domains neglecting the eddy currents [45,49]. Actually, for determining experimentally an hysteresis loop, a bulky specimen is subject to the external applied magnetic field changing with time which is recorded together with the total magnetic moment induced in the sample; the two quantities are plotted and the hysteretic behavior is observed. Therefore the hysteresis loop is a macroscopic observed property of a specific superconducting sample of given dimensions and shape, rather than a constitutive relation of the superconducting materials. The same situation occur when the E-J characteristic is determined through an experimental technique, say the four points one [9]. What is plotted in this case is the course of the voltage as a function of the current over a relatively wide area, which can only approximately be assumed as a local relation among electric field and current density. Indeed, it is not possible to determine a macroscopic constitutive (strictly local) relation directly from experiments, simply because do not exist measuring instruments that operate on the "*point*" scale. However, a constitutive relation in some form can be assumed starting form the experimental data obtained on a specific sample, and can be justified or rejected by examining, through numerical calculations based on this assumption, the behavior of other samples, different for dimensions, shape and operating condition, and comparing the predicted results with the experimental ones. If a good qualitative agreement is always confirmed the comparison of numerical and experimental results can be used to characterize the material, an approach usually followed for deriving the critical current density of superconductors from magnetization measurements, according to the critical state model [6-9]. Likewise, in the following the experimental hysteresis loops measured on bulk samples with a given shape are assumed as constitutive relation of the superconducting material and a justification of the assumption as well as an identification of the loop parameters is provided a posteriori.

The field problem resulting form this schematization can be discretized and numerically solved by means of the model of the equivalent magnetic network described in section 2.2. However, in order to define the parameters of the equivalent magnetic circuit, the local hysteretic M-B characteristic needs to be mathematically specified.

This section is dedicated to the description of the hysteresis model, agreed upon a set of equations which allows a practical fitting of the experimental measured hysteresis loops exhibited by superconducting materials. First we describe a model to reproduce the scalar hysteretic behavior of a superconductor, then we give an extension to the vector hysteresis [50]. We stress that what we describe here is a pure phenomenological model, which do not provide any physical base. The only goal of the model is the definition of the parameters of the equivalent magnetic network on the base of the experimental data. Moreover, in developing the mathematical details, no attempt is made to provide a review of state of art in the mathematical description of hysteresis [40-41].

2.3.1 The scalar hysteresis model

It is an experimental evidence that if a superconducting specimen is subject to an external applied magnetic field **H** which oscillates along a given direction the induced average magnetization **M** follows the resulting magnetic flux density, defined by equation (2.2.1), according to the symmetric hysteretic loop qualitatively shown in figure 2.3.1 [52]. Such an hysteresis cycle, which is said to be *scalar* for the applied field does not change direction, can be completely identified by means of the five parameters which are also shown in the same figure.

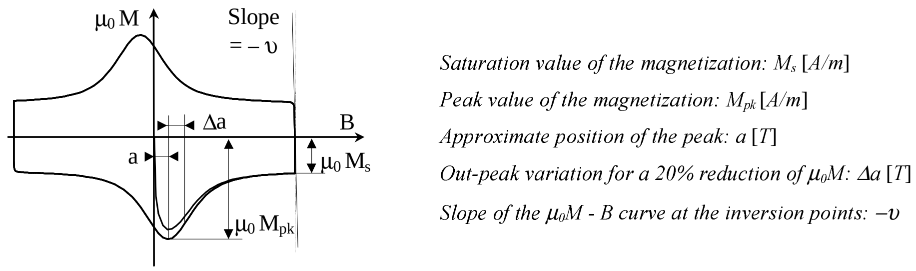

figure 2.3.1: typical scalar hysteresis loop for a superconductor

This loop is supposed to represent the local dependence of **M** on **B**. To account for thermal effects [34], the entire family of hysteresis loop for all temperatures can be considered by assigning a temperature dependence to the five parameters of the loop.

Let us assume that the magnetic flux density oscillates along a given direction **b**, so that the flux density field is expressed as

$$\mathbf{B}(t) = B(t)\mathbf{b} \tag{2.3.1}$$

the point dependence is kept implicit. The initial state, i.e. t = 0, is given by M = B = 0.

During the oscillation the magnetic flux density crosses some inversion points which can be specified by defining the two following sign functions

$$\begin{aligned} \delta^+(t) &= \lim_{\Delta t \to 0+} sgn[B(t+\Delta t) - B(t)] \\ \delta^-(t) &= \lim_{\Delta t \to 0+} sgn[B(t) - B(t-\Delta t)] \end{aligned} \tag{2.3.2}$$

The set of inversion times $\{t_{inv}\}$ and the corresponding set of inversion fields $\{B_{inv}\}$ are defined by

$$\delta^+(t_{inv}) + \delta^-(t_{inv}) = 0 \tag{2.3.3}$$

and

$$B_{inv} = B(t_{inv}) \tag{2.3.4}$$

The set of the inversion times and fields can be placed in an ordered sequence $\{t_{inv_k}, B_{inv_k}\}$. By including conventionally the initial state $(t_{inv\,0}, B_{inv\,0}) = (0,0)$ in the sequence it is possible to define the time evolution of the inversion field by as follow

$$\mathscr{B}_{inv}(t) = B_{inv_k} \qquad if \quad t_{inv_k} \le t < t_{inv_{k+1}} \tag{2.3.5}$$

with k any positive integer.

At any instant the induced magnetization is parallel to the magnetic flux density, i.e.

$$\mathbf{M}(t) = M(t)\mathbf{b} \tag{2.3.6}$$

Let us express the differential increment of the magnetization magnitude with respect to the magnetic flux density by means of the following form of the Duhem type [41]:

$$\mu_0 dM = \begin{bmatrix} f(\mathscr{B}_{inv})\mathscr{F}_s'\left(\dfrac{B-\mathscr{B}_{inv}}{g(\mathscr{B}_{inv})}; a, M_s\right)+ \\ -\mathscr{F}_{pk}'\left(B; \delta^+ a, i_{1st}, \Delta a, M_{pk}, M_s, \beta\right) \end{bmatrix} |dB| \tag{2.3.7}$$

The first term describes the basic behavior, i.e. the saturation, while the second one takes into accounts the peaks. The primes denote differentiation with respect to the first argument, separated by a semicolon. The time dependence is implicit. We assume for function $\mathscr{F}_s$ the following expression

$$\mathscr{F}_s(X; a, M_s) = -\left|\mu_0 M_S \left(coth\left(\frac{X}{a}\right) - \frac{a}{X}\right)\right| \tag{2.3.8}$$

Figure 2.3.2 shows a plot of function $\mathscr{F}_s$. The values of the parameters are also quoted.

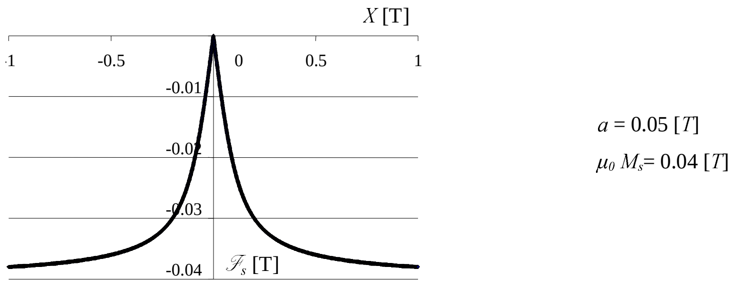

figure 2.3.2: course of function $\mathscr{F}_s$

Notice that function $\mathscr{F}_s$ owns the following properties: it is an even function of X which tends asymptotically to $-\mu_0\ M_s$ as the absolute value of X increases; moreover its derivative respect to X at the origin respect the condition $\mathscr{F}_s(0^{\pm}) \rightarrow \mp(\mu_0 M_S / 3a)$.

Concerning the second contribution $\mathscr{F}_{pk}$ the following expression is assumed

$$\mathscr{F}_{pk}\left(B;\delta^{+}a, i_{1st}, \Delta a, M_{pk}, M_s, \beta\right) =$$

$$= \begin{cases} \mu_0\left(\beta M_{pk} - M_s\right)\begin{cases} \sqrt{1-\left(1-\left|\dfrac{B}{a}\right|\right)^2} & , if \quad |B| < |a| \\ 3\left[1 - coth^2\left|\dfrac{|B|-|a|}{\Delta a}\right| + \left(\dfrac{\Delta a}{|B|-|a|}\right)^2\right] & , if \quad |B| > |a| \end{cases} & , if \quad i_{1st} = 1 \\ 3\mu_0\left(M_{pk} - M_s\right)\left[1 - coth^2\left|\dfrac{B-a}{\Delta a}\right| + \left(\dfrac{\Delta a}{B-a}\right)^2\right] & , if \quad i_{1st} = 0 \end{cases}$$

(2.3.9)

The time dependent index i_{1st}, defined by equation (2.3.10), discriminates if, at the current instant, the cycle lies on the first magnetization curve or if it has yet crossed an inversion point.

$$i_{1st}(t) = \begin{cases} 1 & ,if \quad \mathscr{B}_{inv}(\tau) = 0, \forall \tau \in [0,t] \\ 0 & ,if \quad \exists \tau \in [0,t] \mid \mathscr{B}_{inv}(\tau) \neq 0 \end{cases} \tag{2.3.10}$$

β is a reduction factor (if needed) for the first magnetization curve. Figure 2.3.3 shows the course of the given $\mathscr{T}_{pk}$ function with $a = \Delta a = 0.05$ T, $\mu_0 M_{pk} = 0.12$ T, $\mu_0 M_s = 0.04$ T, $\beta = 1$ for both the cases $i_{1st} = 0$ and $i_{1st} = 1$.

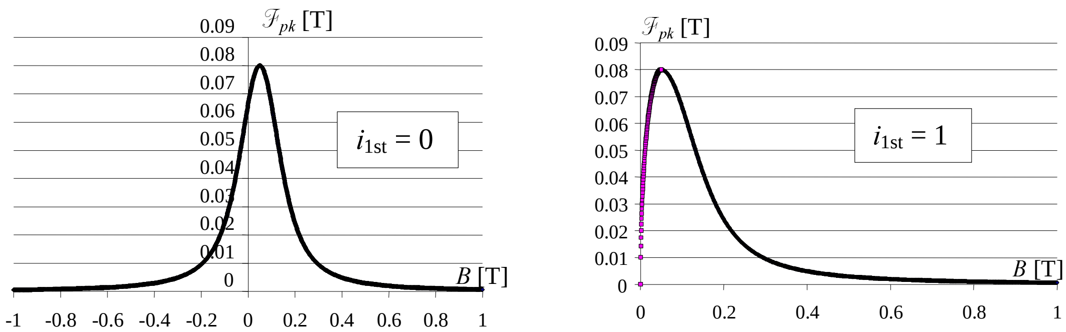

figure 2.3.3:course of function $\mathscr{T}_{pk}$

Notice that function $\mathscr{T}_{pk}$ owns the following properties: $\mathscr{T}_{pk}(-B, -a, 1) = \mathscr{T}_{pk}(B, a, 1)$, $\mathscr{T}_{pk}(0, a, 1) = 0$, $\mathscr{T}_{pk}'(0, \pm a, 1) \to \pm\infty$, $\mathscr{T}_{pk}(a - B, a, 0) = \mathscr{T}_{pk}(a + B, a, 0)$, and $\mathscr{T}_{pk}(\pm\infty, a, i_{1st}) \to 0$.

It is a well established feature of the hysteresis that the current value of the induced magnetization depends only the set of values of the magnetic flux density at all the inversion points, which is usually referred to as a *complete memory set* (*CMS*) of *B*, and not on the complete history of *B* [40]. A generic magnetized state which satisfies this condition can be indicated thorough the Enderby notation [53], i.e.

$$M(B) = M\left({}_{0}{}^{B_{inv,1}}{}_{B_{inv,2}} \cdots {}^{B_{inv,n-1}}{}_{B_{inv,n}}{}^{B}\right) \tag{2.3.11}$$

With notation (2.3.11) we also state that only the values of inversion field, and not the corresponding instants, determine the magnetized state. This property is referred to as *rate independence* of the hysteresis. The generic B_{inv_i} denotes an inversion point that ends an increasing piece of the cycle if it is in an upper position while it ends a decreasing one if it lies in a lower position.

In order to specify functions *f* and *g* of equation (2.3.7) we now impose the following requirements on the hysteresis curves:

i) the magnetization process of a virgin point must be independent from the sign of d*B*, i.e. $M\left({}^{0}{}_{-B}\right) = -M\left({}_{0}{}^{B}\right)$.

ii) At the initial state $M = B = 0$ the condition $\mathrm{d}M/\mathrm{d}B \to -\infty$ must be respected to take account of the Meissner effect at low fields.

iii) if $|B|$ increases without bound *M* reaches a positive or negative saturation value (depending on whether *B* decrease or increases) which is independent from the set of the preceding inversion points, i.e. $M\left(\cdots^{+\infty}\right) = -M_s$ and $M\left(\cdots_{-\infty}\right) = +M_s$.

iv) immediately after an inversion point $\mu_0\, \mathrm{d}M/\mathrm{d}B = -\upsilon$, with $\upsilon >> 1$.

Let us now consider the time interval $\left[0, t_{inv_1}\right]$ where the magnetic flux density is monotone, e.g. increasing. Since in the given time interval $\mathscr{B}_{inv}(t) = 0$, equation (2.3.7) can be expressed as

$$\mu_0\, dM = \delta^{+}\left[f(0)\mathscr{F}_s{}'\left(\frac{B}{g(0)}\right) - \mathscr{F}_{pk}'\left(B; \delta^{+} a, i_{1st}\right)\right] dB \qquad (2.3.12)$$

where the dependence of functions $\mathscr{F}_s$ and $\mathscr{F}_{pk}$ on the parameters of the cycle Δa, $\mu_0 M_{pk}$, $\mu_0 M_s$, and β is implicit. By integrating equation (2.3.12) over the considered time interval it follows

$$\mu_0 M\left({}_0^{B}\right) = \delta^+\left[f(0)g(0)\mathscr{F}_s\left(\frac{B}{g(0)}\right) - \mathscr{F}_{pk}\left(B;\delta^+ a, i_{1st}\right)\right] \tag{2.3.13}$$

where i_{1st} = 1 and δ^+ = 1. By exploiting the properties of functions $\mathscr{F}_s$ and $\mathscr{F}_{pk}$ we find, by direct inspection on equations (2.3.13) and (2.3.12) respectively, that requirement (i) and (ii) are satisfied whatever are the value of $f(0)$ and $g(0)$. Moreover, by letting the absolute value of magnetic flux density to increase monotonically without bound and considering equation (2.3.13) together with the properties of $\mathscr{F}_s$ and $\mathscr{F}_{pk}$ we find that, for the requirement (iii) to be satisfied the following condition must hold

$$-\delta^+\mu_0 M_s = -\delta^+ f(0)g(0)\mu_0 M_s \tag{2.3.14}$$

therefore the value $g(0)$ can be expressed as a function of $f(0)$ as follow

$$g(0) = \frac{1}{f(0)} \tag{2.3.15}$$

Let us now suppose that, starting form the generic inversion point $\left(t_{inv_i}, B_{inv_i}\right)$, with e.g. a positive value, the magnetic flux decreases up to the next inversion point $\left(t_{inv_{i+1}}, B_{inv_{i+1}}\right)$, and then increases. We denote the induced magnetization at the inversion point with $M_{inv_i} = M\left({}_0 \cdots^{B_{inv_i}}\right)$. By considering equation (2.3.7) over the time interval $\left[t_{inv_i}, t\right]$, with $t > t_{inv_i}$, since $\mathscr{B}_{inv}(t) = B_{inv_i}$

$$\mu_0 dM = \delta^+\left[f\left(B_{inv_i}\right)\mathscr{F}_s'\left(\frac{B-B_{inv_i}}{g\left(B_{inv_i}\right)}\right)-\mathscr{F}_{pk}'\left(B;\delta^+a,i_{1st}\right)\right]dB \qquad (2.3.16)$$

where i_{1st} = 0. By integrating equation (2.3.16) and considering the properties of functions $\mathscr{F}_s$ and $\mathscr{F}_{pk}$, we obtain

$$\begin{aligned}&\mu_0 M\left({}_0\cdots^{B_{inv_i}}{}_B\right)=\mu_0 M_{inv_i}+\\&+\delta^+\left[f\left(B_{inv_i}\right)g\left(B_{inv_i}\right)\mathscr{F}_s\left(\frac{B-B_{inv_i}}{g\left(B_{inv_i}\right)}\right)-\mathscr{F}_{pk}\left(B;\delta^+a,i_{1st}\right)+\mathscr{F}_{pk}\left(B_{inv_i};\delta^+a,i_{1st}\right)\right]\end{aligned} \qquad (2.3.17)$$

From equation (2.3.16) it follows

$$\mu_0\left.\frac{dM}{dB}\right|_{B\to B_{inv_i}^-}=\delta^+\left[f\left(B_{inv_i}\right)\frac{\mu_0 M_S}{3a}-\mathscr{F}_{pk}'\left(B_{inv_i};\delta^+a,i_{1st}\right)\right] \qquad (2.3.18)$$

and consequently, from the requirement (iv) it follows that $f\left(B_{inv_1}\right)$ can be calculated as

$$f\left(B_{inv_i}\right)=\frac{3a}{\mu_0 M_S}\left[-\delta^+\upsilon+\mathscr{F}_{pk}'\left(B_{inv_i};\delta^+a,i_{1st}\right)\right] \qquad (2.3.19)$$

Indeed the peak of function $\mathscr{F}_{pk}$, which occurs for B = a in the case where an inversion is yet occurred (i_{1st} = 0), is quite narrow (see figure 2.3.3). Therefore if the condition $(B/a)>>1$ holds, equation (2.3.19) can be conveniently approximated as

$$f\left(B_{inv_1}\right)=-\delta^+\frac{3a\upsilon}{\mu_0 M_s} \qquad (2.3.20)$$

Moreover, if B decreases without bound requirement (iii) imposes that

$$\mu_0 M_s = \mu_0 M_{inv_i} - \delta^+ f\left(B_{inv_i}\right) g\left(B_{inv_i}\right)\mu_0 M_s + \delta^+ \mathscr{I}_{pk}\left(B_{inv_i}; \delta^+ a, i_{1st}\right) \qquad (2.3.21)$$

therefore the values of $f\left(B_{inv_1}\right)$ and $g\left(B_{inv_1}\right)$ are not independent and satisfies the condition

$$g\left(B_{inv_i}\right) = \frac{1}{\delta^+ f\left(B_{inv_i}\right)}\left[-1 + \frac{\mu_0 M_{inv_i} + \delta^+ \mathscr{I}_{pk}\left(B_{inv_i}; \delta^+ a, i_{1st}\right)}{\mu_0 M_s}\right] \qquad (2.3.22)$$

Now it easy to demonstrate that equations (2.3.15) and (2.3.20) and (2.3.22) can be generalized to

$$f\left(\mathscr{B}_{inv}(t)\right) = -\delta^+ \frac{3a\upsilon}{\mu_0 M_s} \qquad (2.3.23)$$

and

$$\begin{aligned} & g\left(\mathscr{B}_{inv}(t)\right) = \\ & = \frac{1}{f\left(\mathscr{B}_{inv}(t)\right)}\left[-\delta^+(t) + \delta^+(t)\frac{\mu_0 \mathscr{M}_{inv}(t) + \delta^+(t)\mathscr{I}_{pk}\left(\mathscr{B}_{inv}(t); \delta^+(t)a, i_{1st}(t)\right)}{\mu_0 M_s}\right] \end{aligned} \qquad (2.3.24)$$

where function $\mathscr{M}_{inv}(t)$ is defined as follow

$$\mathscr{M}_{inv}(t) = M_{inv_k} \qquad if \quad t_{inv_k} \le t < t_{inv_{k+1}} \qquad (2.3.25)$$

Equations (2.3.23) and (2.3.24) completely define the hysteresis model (2.3.7). By integrating the latter over a time interval [t^{old}, t^{new}] such that during it the inversion index $\delta^{+}(t)$ does not change, the updated magnetic state can be determined on the base of the outdated one as follows

$$\mu_0 M^{new} = \mu_0 M^{old} + \\ + \delta^{+}\left(t^{new}\right)\left[\begin{array}{c} f\left(\mathscr{B}_{inv}\left(t^{new}\right)\right) g\left(\mathscr{B}_{inv}\left(t^{new}\right)\right) \mathscr{F}_s\left(\dfrac{B^{new} - \mathscr{B}_{inv}\left(t^{new}\right)}{g\left(\mathscr{B}_{inv}\left(t^{new}\right)\right)}\right) + \\ + \mathscr{F}_{pk}\left(B^{new}; \delta^{+}\left(t^{new}\right) a, i_{1st}\left(\left(t^{new}\right)\right)\right) - \mathscr{F}_{pk}\left(B^{old}; \delta^{+}\left(t^{new}\right) a, i_{1st}\left(t^{old}\right)\right) \end{array}\right] \tag{2.3.26}$$

It the course of the magnetic flux density is provided equation (2.3.19), which can be easily numerically implemented, allows to calculate the hysteresis loop on the base only of the five parameters a, M_s, Δa, M_{pk} and υ, which must be assigned. Figure 2.3.4 shows the calculated hysteresis loop of a material characterized by a = 0.1 T, $\mu_0\ M_s$ = 0.04 T, Δa = 0.1 T, $\mu_0\ M_{pk}$ = 0.12 T, β = 0.9 and υ = 100, subject to a magnetic flux density which oscillates with an amplitude of 1 T. Figure 2.3.5 shows the calculated hysteresis loop of the same material subject to a magnetic flux density which oscillates with a continuously increasing an amplitude.

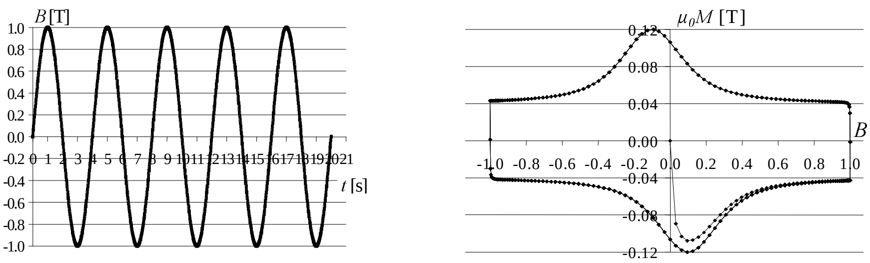

figure 2.3.4: hysteresis loop for an oscillating field

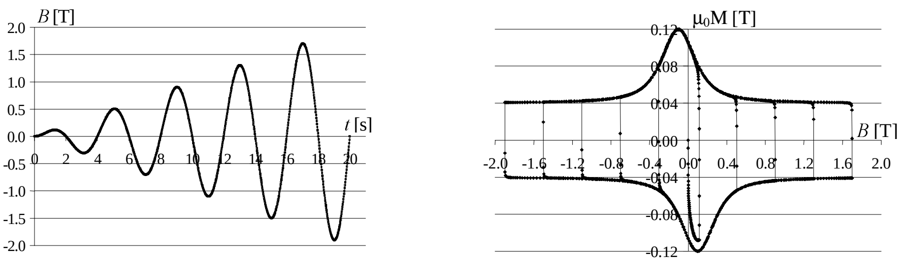

figure 2.3.5: hysteresis loop for a field oscillating with increasing amplitude

2.3.2 The vector hysteresis model

Let us consider an isotropic superconductor subject to a magnetic flux density whose magnitude and direction can change with time expressed as

$$\mathbf{B}(t) = B(t)\mathbf{b}(t) \tag{2.3.27}$$

where **b** is a time dependent unit vector. The induced magnetization at any instant has also time varying magnitude and direction and is expressed as

$$\mathbf{M}(t) = M(t)\mathbf{m}(t) \tag{2.3.28}$$

where **m** is a time dependent unit as well. Let us first consider the case of rotating magnetic flux density with constant magnitude. An isotropic superconductor subject to an uniformly rotating magnetic flux density **B** experiences an uniformly rotating magnetization **M** that lags behind it by some constant angle which depends on the magnitude of vector **B** [54]. Our goal is to define mathematically the dependence of vector **M** on **b**. Let us introduce the lag angle ϑ_L defined as the angle between the unit vectors **b** and **m**; in general this angle can be equal or displaced by π respect to the to the angle between the physical vector **M** and **B** as shown in figure 2.3.6.

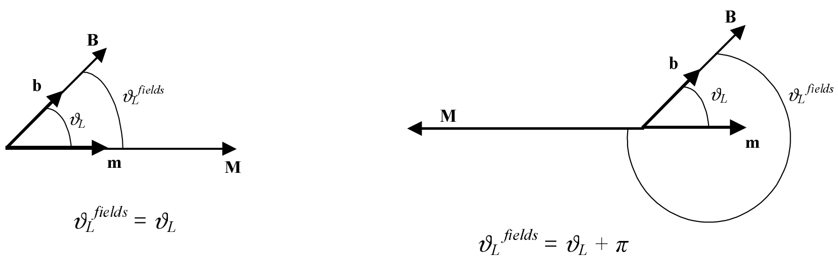

figure 2.3.6: lag angle

Let us assume that for some reason at a certain instant the angular displacement ϑ among vectors **b** and **m** can be out of the equilibrium value ϑ_L; the generic ϑ can be expressed as

$$\vartheta = arccos(\mathbf{m} \cdot \mathbf{b}) \qquad (2.3.29)$$

We now suppose that at a variation d**b** of the direction of the magnetic flux density occurs, causing a change of the angle among **b** and **m**, as schematized in figure 2.3.7, where the top scripts *old* and *new* denote the quantities before and after the variation.

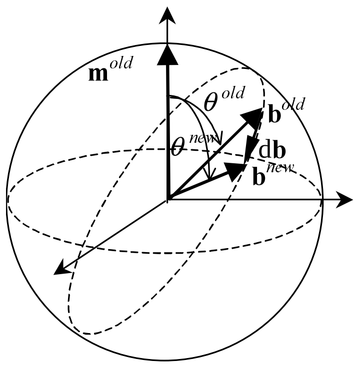

figure 2.3.6: infinitesimal change of direction of the magnetic flux density

Following d**b** the angle ϑ^{new} among **m** and **b** becomes

$$\vartheta^{new} = arccos(\mathbf{m}^{old} \cdot \mathbf{b}^{new}) \qquad (2.3.29)$$

Note that vectors $\mathbf{b}^{old}$, $\mathbf{b}^{new}$ and $\mathbf{m}^{old}$ may not lie on the same plane. Let us now assume that the direction $\mathbf{m}^{new}$ of the new magnetization lies on the arc connecting $\mathbf{m}^{old}$ to $\mathbf{b}^{new}$ and express it through the following equation

$$\mathbf{m}^{new} = \alpha\left(\xi\left(\vartheta^{new}, \vartheta^{new} - \vartheta^{old}; \vartheta_L, \Delta\vartheta_c\right), \mathbf{m}^{old}, \mathbf{b}^{new}\right) \qquad (2.3.30)$$

where $\Delta\vartheta_c$ is a parameters named interaction angle which will be defined in a moment. We assume for function α the following expression

$$\alpha(\xi,\mathbf{m},\mathbf{b})=\mathbf{m}cos\xi+\frac{\mathbf{b}-\mathbf{m}(\mathbf{b}\cdot\mathbf{m})}{\sqrt{1-(\mathbf{b}\cdot\mathbf{m})^2}}sen\xi \tag{2.3.31}$$

where the variable ξ, which is related to the old and the new angular displacement, can assume any value within the interval [0, π]. Function α owns the following properties: $|\alpha(\xi,\mathbf{m},\mathbf{b})|=1$, $\alpha(0,\mathbf{m},\mathbf{b})=\mathbf{m}$ and $\alpha(arccos(\mathbf{m}\cdot\mathbf{b}),\mathbf{m},\mathbf{b})=\mathbf{b}$. In order to specify the variable ξ we impose the following requirements

v) if ϑ is equal to zero (within a given tolerance) then the small deviation from the parallelism between $\mathbf{m}^{old}$ and $\mathbf{b}^{new}$ do not affect $\mathbf{m}^{new}$, therefore, according to the second property of function α, ξ must approach zero

vi) if $\vartheta > \vartheta_L$ then vector $\mathbf{m}^{new}$ tends to follow $\mathbf{b}^{new}$ in order to keep unchanged the angular displacement ($\mathbf{m}^{new}-\mathbf{b}^{new}\rightarrow\ \mathbf{m}^{old}-\mathbf{b}^{old}$), therefore, according to the third property of function α, ξ must approach $\vartheta^{new}-\vartheta^{old}$

For expressing quantitatively these properties we introduce the fuzzy function $\mathscr{g}$ defined as

$$\mathscr{g}(\omega)=\begin{cases}0 & ,if\ \omega<-1\\ \frac{1}{2}+\frac{3}{4}\omega-\frac{1}{4}\omega^3 & ,if\ |\omega|\le+1\\ 1 & ,if\ \omega>+1\end{cases} \tag{2.3.32}$$

The course of function $\mathscr{g}$ is represented in figure 2.3.7

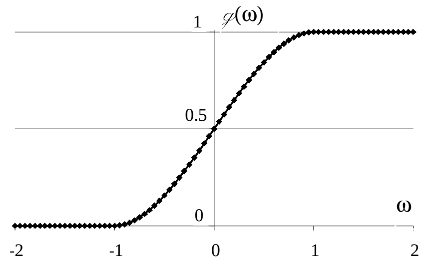

figure 2.3.7: course of function $\mathscr{g}$

Therefore, according to requirements (v) and (vi) the variable ξ can be defined as follow

$$\xi(\vartheta, \Delta\vartheta; \vartheta_L, \Delta\vartheta_c) = \mathscr{g}\left(\frac{\vartheta - \vartheta_L + \Delta\vartheta_c}{\Delta\vartheta_c}\right)\Delta\vartheta \tag{2.3.33}$$

Now, the meaning of the interaction angle $\Delta\vartheta_c$ is clear: if $\vartheta > \vartheta_L$ then $\xi = \Delta\vartheta = \vartheta^{new} - \vartheta^{old}$, so that the angular distance between **m** and **b** remains unchanged, whereas if $\vartheta < \vartheta_L - \Delta\vartheta_c$ then $\xi = 0$, so that small deviation from the parallelism between $\mathbf{m}^{old}$ and $\mathbf{b}^{new}$ does not affect $\mathbf{m}^{new}$.

Equations (2.3.30) and (2.3.33) can be seen as the discretized version of the following differential model:

$$d\mathbf{m} = \begin{cases} 0 & , if \;\; \mathbf{m} = \mathbf{b} \\ \dfrac{\mathbf{b} - \mathbf{m}(\mathbf{b}\cdot\mathbf{m})}{\sqrt{1-(\mathbf{b}\cdot\mathbf{m})^2}}\, d\hat{\xi} & , if \;\; \mathbf{m} \neq \mathbf{b} \end{cases} \tag{2.3.34}$$

and

$$d\hat{\xi} = \mathscr{g}\left(\frac{\vartheta - \vartheta_L + \Delta\vartheta_c}{\Delta\vartheta_c}\right) d\vartheta \tag{2.3.35}$$

Notice that this model guarantees the condition $\mathbf{m}\cdot d\mathbf{m} = 0$.

Figure 2.3.8 shows the behavior of the magnetization calculated through equations (2.3.26), (2.3.30) and (2.3.33) for a material having a = 0.1 T, $\mu_0 M_s$ = 0.04 T, Δa = 0.1 T, $\mu_0 M_{pk}$ = 0.12 T, β = 0.9, υ = 100, ϑ_L = 11π/36 (55°) and $\Delta\vartheta_c$ = π/36 (5°) subject to a magnetic flux density rotating in the *x*-*y* plane with an amplitude of 1 T. The initial zero value interval for the *x* component is essential because the starting configuration must always be the $M = B = 0$ point.

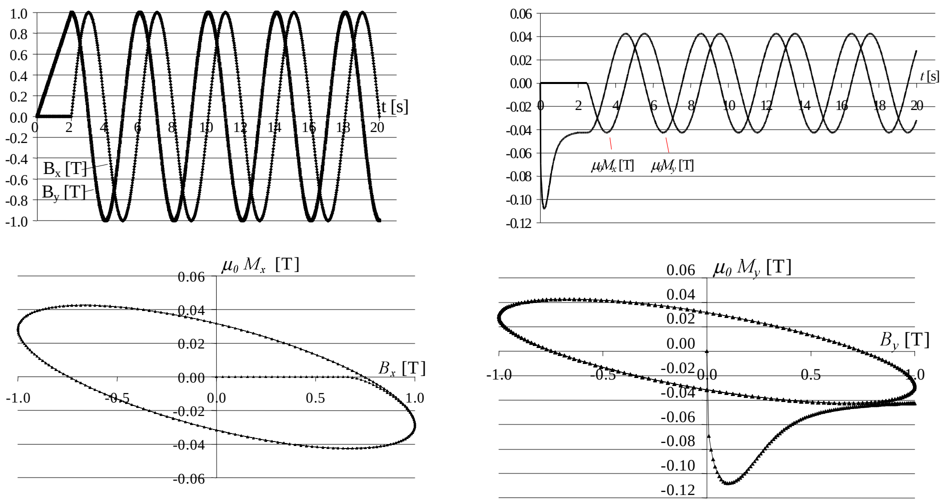

figure 2.3.8: magnetization induced by a rotating field

In order to complete our hysteresis model we have to face now the case where both the direction and the magnitude of the magnetic flux density can change. For defining the inversion points, which in this case is not a trivial task, let us introduce the following function

$$\sigma(t) = \lim_{\Delta t \to 0^+} \frac{\mathbf{B}(t+\Delta t)\cdot \mathbf{B}(t-\Delta t)}{|\mathbf{B}(t+\Delta t)|\,|\mathbf{B}(t-\Delta t)|} \qquad (2.3.36)$$

Since, due to the fact that **B**(t) is not defined for t < 0, function σ is not defined in t = 0, we extend it to this point by assigning $\sigma(0) = -1$. Provided that **B**(t) is a continuous function, i.e. both functions $B(t)$ and **b**(t) of equation (2.3.27) are continuous, and considering that **b**(t) is a time dependent unit vector, equation (2.3.37) becomes

$$\sigma(t) = \lim_{\Delta t \to 0^+} \frac{B(t+\Delta t)B(t-\Delta t)}{|B(t+\Delta t)|\,|B(t-\Delta t)|} \tag{2.3.37}$$

It follows that σ can be different from 1 only in for a numerable set of instants in which function $B(t)$ crosses the zero. Equation (2.3.37) enlarge to the case of vector hysteresis the definition of inversion point given by equations (2.3.2) for the scalar case. The inversion instants $\{t_{inv}\}$ are then defined by the condition

$$\sigma(t_{inv}) = -1 \tag{2.3.38}$$

which replace condition (2.3.3) suitable for the scalar hysteresis. The inversion fields $\{B_{inv}\}$ are still defined bye equation (2.3.4). The set of the inversion times and fields can be placed in an ordered sequence $\{t_{inv_k}, B_{inv_k}\}$ which includes also the initial state. The time evolution of the inversion field is defined by equation 2.3.5.

We now introduce an inversion index $i_{inv}(t)$ defined as follow

$$i_{inv}(t) = (-1)^k, \qquad for\ \ t_{inv_k} \le t < t_{inv_{k+1}} \tag{2.3.39}$$

This inversion index can be used to introduce the following definitions

$$B(t) = i_{inv}(t)|\mathbf{B}(t)| \tag{2.3.40}$$

and

$$\mathbf{b}(t) = \begin{cases} \lim\limits_{\Delta t \to 0^+} i_{inv}(t-\Delta t)\dfrac{\mathbf{B}(t-\Delta t)}{|\mathbf{B}(t-\Delta t)|} & ,if\ \ \mathbf{B}(t) = 0 \\ i_{inv}(t)\dfrac{\mathbf{B}(t)}{|\mathbf{B}(t)|} & ,if\ \ \mathbf{B}(t) \neq 0 \end{cases} \tag{2.3.41}$$

Notice that the condition **B**(t) = B(t) **b**(t) is maintained through these relations.

Let us now consider a small but finite time increment Δt such that through it vector **B**(t) changes but no inversions occur, i.e. function $\sigma(t)$ assumes only value 1; by denoting with the top scripts *old* and *new* the quantities at the beginning and at the end of the time increment we can express the updated magnetic flux density on the base of the outdated one by using the following discretized form of equations (2.3.39) – (2.3.41)

$$i_{inv}^{new} = \begin{cases} -i_{inv}^{old} & , if \quad \mathbf{B}^{new} \cdot \mathbf{B}^{old} \le 0 \\ i_{inv}^{old} & , if \quad \mathbf{B}^{new} \cdot \mathbf{B}^{old} > 0 \end{cases} \tag{2.3.42}$$

$$B^{new} = i_{osc}^{new} \left| \mathbf{B}^{new} \right| \tag{2.3.43}$$

$$\mathbf{b}^{new} = \begin{cases} \mathbf{b}^{old} & , if \;\; \mathbf{B}^{new} = 0 \\ i_{osc}^{new} \dfrac{\mathbf{B}^{new}}{\left| \mathbf{B}^{new} \right|} & , if \;\; \mathbf{B}^{(new)} \ne 0 \end{cases} \tag{2.3.44}$$

Now that functions $B(t)$ and **b**(t) are clearly defined we can apply equations (2.3.26) and (2.3.30) to calculate the time evolution of the induced magnetization. Notwithstanding we must observe that the vector hysteresis model (equations (2.3.30)-(2.3.33)) is capable, by construction, to give a continuous time evolution of the magnetization only if vector **b**(t) experiences smooth variations. In the case where dB ≠ 0 however, due to equation (2.3.44), a large variation of ϑ can occur and the calculated magnetization can be discontinuous. Therefore the model so far defined cannot be used to consistently predict what happen if a non-uniform rotation is experienced by the material. In order to overcome this impasse an extension of the vector hysteresis model to the case where dB ≠ 0 is required. The simplest way to accomplish this task is to generalize its differential form (equation (2.3.35)) as follow

$$d\hat{\xi} = \mathscr{T}(t)\mathscr{G}\left(\frac{\vartheta - \vartheta_L + \Delta\vartheta_c}{\Delta\vartheta_c} \right) d\vartheta + \left| \frac{\partial\alpha}{\partial B} dB \right| \tag{2.3.45}$$

In order to let equation (2.3.45) coincide with equation (2.3.35) in case of uniform rotation ($dB = 0$, $\sigma(t) = 1$, $\forall\ t > 0$) we can define function $\mathscr{F}$ as follow

$$\mathscr{F}(t) = \begin{cases} 1 & , if \quad \sigma(t) = 1 \\ 0 & , if \quad \sigma(t) = -1 \end{cases} \tag{2.3.46}$$

If we are interested in dealing with continuous functions we can alternatively define function $\mathscr{F}$ as $\mathscr{F}(t) = \mathscr{G}\left(1 + \frac{\sigma(t) - 1}{\Delta\sigma}\right)$, where $\Delta\sigma$ is a parameter having a small value.

The function α is introduced in equation (2.3.45) to take account of the demagnetizing effect of the magnetic field with on a mutually orthogonal component of magnetization. In fact, it an experimental evidence that when a magnetic field is first applied along a certain direction **m** and then removed a non zero component M^0_m of magnetization remains along that direction. If subsequently the magnetic field is increased along an orthogonal direction **b** the former component of magnetization decreases and vanishes as the magnetic field increases [54,55], as schematically shown in figure 2.3.9. An analog behavior is observed also when **m** and **b** are not orthogonal.

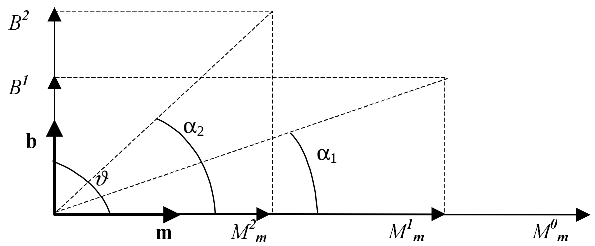

figure 2.3.9: correlation between mutually orthogonal component vectors **M** *and* **B**

From the figure it is evident that the angles α_1 and α_2, which depend on both the magnitudes of magnetization and magnetic flux density and on the angle ϑ , are parameter which gives a significative account of the demagnetizing effect, therefore function α can be expressed as

$$\alpha = \alpha(B, M, \vartheta) = arctan\left(\frac{|B| sen\vartheta}{|M| + |B| cos\vartheta}\right) \tag{2.3.46}$$

Notice that the differential form (2.3.45) is not an exact differential since the integrability condition is not respected. This means that ξ is not a function of ϑ and B and (29) has a meaning only if the time dependence of **B** is specified.

By considering again a small but finite time increment Δt such that through it vector **B**(t) changes but no inversions occur, the following equation for the variation is obtained

$$\begin{aligned} \xi = {} & \mathcal{F}\mathcal{G}\left(\frac{\vartheta^{new} - \vartheta_L + \Delta\vartheta_c}{\Delta\vartheta_c}\right)\left(\vartheta^{new} - \vartheta^{old}\right) + \\ & + \left|\alpha\left(B^{new}, M^{old}, \vartheta^{new}\right) - \alpha\left(B^{old}, M^{old}, \vartheta^{old}\right)\right| \end{aligned} \tag{2.3.47}$$

Moreover, we specify $\mathcal{F}$ as follows

$$\begin{aligned} \mathcal{F} = {} & 1 - \mathcal{G}\left(2\frac{\left|\vartheta^{new} - \vartheta^{old}\right| - \Delta\vartheta_c}{\Delta\vartheta_c}\right) + \\ & + \mathcal{G}\left(2\frac{\left|\vartheta^{new} - \vartheta^{old}\right| - \Delta\vartheta_c}{\Delta\vartheta_c}\right) \mathcal{Y}\left(\frac{B^{new} - B^{old}}{\Delta B_L}\right) \end{aligned} \tag{2.3.48}$$

where the function $\mathcal{Y}$ is defined as follows

$$\mathcal{Y}(\omega) = \begin{cases} 0 & , if\ |\omega| > +1 \\ \left(1 - \omega^2\right)^2 & , if\ |\omega| \le +1 \end{cases} \tag{2.3.49}$$

The course of function $\mathcal{Y}$ is represented in figure 2.3.10

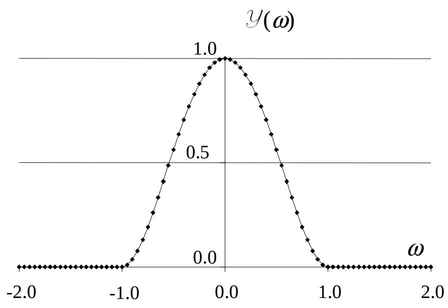

figure 2.3.10: course of function $\mathcal{Y}$

Through equation (2.3.48) an inversion instant, identified by the condition $\mathcal{F} = 0$, is detected if and only if $\mathcal{Y}(\Delta B/\Delta B_L) = 0$ and $g\,(2(|\Delta\vartheta| - \vartheta_{L+})/\Delta\vartheta_c) = 1$. These conditions are met if and only if $|\Delta B| > \Delta B_L$ and $|\Delta\vartheta| > 3\ \Delta\vartheta|_c\ /2$. The positive parameter ΔB_L labeled "activation field for large-scale swirling" results to be fundamental to discriminate between rotations and free variations. Finally, note then if $B^{new} = B^{old}$ then $\mathcal{F} = 1$ and e.q (2.3.47) coincides with (2.3.33).

Equations (2.3.26), (2.3.30) and (2.3.47) form the complete hysteresis model, i.e. they allow the calculate the time evolution of the induced magnetization when the time evolution of the anyhow changing magnetic flux density is provided.

Figure (2.3.11) shows the hysteresis curve calculated by means of the complete model for a material having $a = 0.1$ T, $\mu_0 M_s = 0.04$ T, $\Delta a = 0.1$ T, $\mu_0 M_{pk} = 0.12$ T, $\beta = 0.9$, $\upsilon = 100$, $\vartheta_L = 11\pi/36$ (55°) and $\Delta\vartheta_c = \pi/36$ (5°) and $\Delta B_L = 0.012$ T, subject to a magnetic flux density that is first pulsed in the y-direction and then oscillates in the x-direction

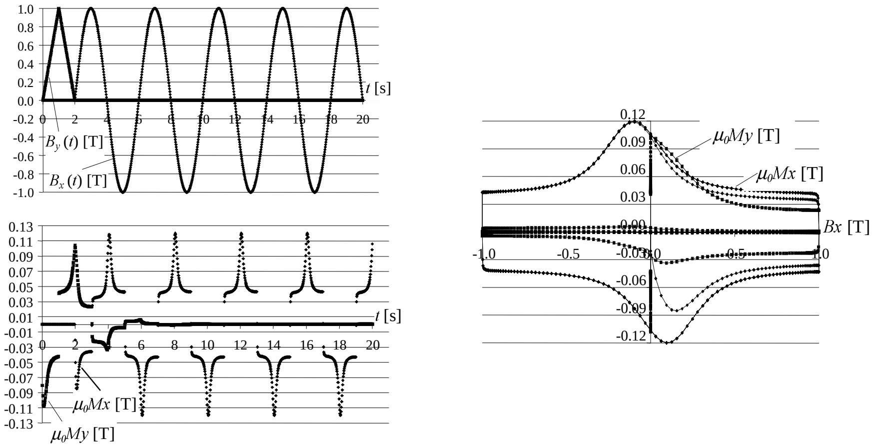

figure 2.3.11: the hysteresis curve for a field pulsed along y and oscillating along x

2.4 Numerical analysis of the Pulsed Field Magnetization of YBCO rings

It has been experimentally established that, due to their very high critical current density, bulk type YBCO superconductors prepared using melt texturing processes can trap magnetic fields beyond 14 T [56,57]. Due to this very high remanence these materials emerge as very interesting for cryo-permanent magnet applications. There exist two techniques to magnetize an SC bulk: the field cooling (FC) and the pulsed field magnetization (PFM). In the former case a strong DC magnetic field produced by a large superconducting coil is first applied and maintained until the superconductor is cooled down below its critical temperature in order to trap the applied field. In the latter case the superconductor is subject to an intense pulsed field produced by a small copper coil which magnetize it and a magnetic field remains trapped after the pulse expiration due to the hysteresis [58,62]; this technique is ideal for fast and *in situ* magnetization. However since the assembly of electrical devices having magnetized parts is very difficult an *in situ* magnetization is desirable [49,63] and the pulsed field technique results favorable. Moreover, the PFM technique can also be used to recover partial demagnetization produced by anomalous events such as short circuits or temperature increases.

To fully magnetize a zero field cooled superconductor under stationary conditions, according to the Bean critical state model the applied magnetic field must be increased up to about twice the saturation field. Moreover, if the magnetization process is fast (as in the case of PFM) strong shielding effects arise [61] and a pulse peak larger than twice the saturation field is required to accomplish full magnetization. In addition, it is proved that the profile of the trapped flux has a strong effect on the performance of the device which lodges the cryo-permanent magnet. Thus, in order to take account of these practical constrains, an improved understanding of the dynamics of the pulsed field magnetization process, both by experimental testing and numerical modeling, is required.

It has been reported by Fabbri *et al* [62] that E-J power law based finite element calculations, for the prediction of the field trapped by a ring shaped YBCO bulk subject to pulsed magnetization, allow a good agreement with the experimental results as long as the field trapped over above and out from the ring concerned, whereas a significant overestimation is observed for the field trapped over the ring hole[2]. Contrariwise, it is important to notice that a good overall agreement is reported in the literature between experimental and numerical results based on the E-J power law, in case of disk shaped samples subject to pulsed magnetization [58].

Actually, even by resorting to qualitative reasoning, the experimental observed fall of the trapped magnetic field above the hole of ring shaped samples seems hard to be predicted by an E-J power law based numerical model, therefore the intent to perform the same calculation by using a model which assumes the experimental M-B hysteresis curve (in the limit where it can be assumed as a local relation, as discussed at the beginning of section 2.3) instead of the power law as constitutive relation, is motivated; this approach is legitimated by the fact that, if it is only deducted by measuring the magnetic field outside, the diamagnetic behavior of a superconductor can be modeled through an induced magnetization rather than an induced of currents. The E-J and the M-B models are found to be equivalent when simply connected geometries are considered, in fact in this case the experimental measured M-B hysteresis loops are well reproduced numerically if the E-J power law is assumed as constitutive relation.

After this premise we now proceed to see how the model of the equivalent magnetic network described in section 2.2, which does assume the experimental hysteresis curve as constitutive relation, reproduces the profile of field trapped by a ring shaped superconducting bulk subject to pulsed magnetization. The thermal effects are not taken in account, i.e. the whole SC bulk is supposed to be in thermal equilibrium with the assigned temperature of 77 K and the experimental hysteresis curve assumed as constitutive relation refers to this temperature.

The numerical results shown below are calculated with reference to the experimental apparatus used by Fabbri *et al.* [62], consisting of a zero field cooled YBCO ring subject to the pulsed field produced by a split Helmotz coil. A scheme of the apparatus is shown in figure 2.4.1. The dimension of the YBCO ring are also quoted in the figure.

---

[2] The same calculation performed with the model of the equivalent electrical network described in section 1.2, which also uses the E-J power law as constitutive relation for the superconductor, gives results coincident with those of [62].

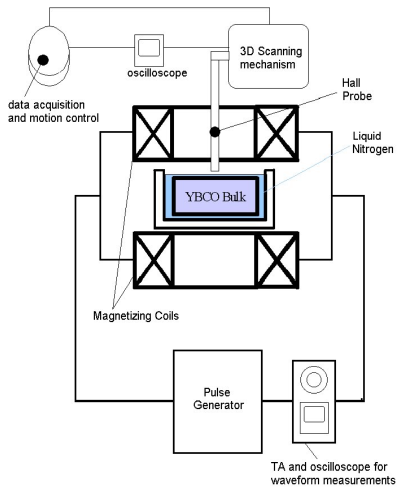

YBCO ring dimension*:*

Inner Radius R_i = 8 *mm*

Outer Radius R_o = 8 *mm*

Eight s = *15 mm*

figure 2.4.1: scheme of the experimental apparatus

The two Helmotz windings are placed symmetrically respect to the superconducting sample at a distance of 117 mm one from the other and are supplied, through the controlled discharge of a capacitors bank, in a way to produce a symmetric magnetic flux density pulse having 0.9 *T* peak and 6 *ms* duration. The axial and the radial components of the magnetic flux density produced by the coil at t = 3 *ms* (peak instant) when the ring is not inserted are shown in Figure 2.4.2. A cylindrical coordinate frame, having the origin in the middle plane and the z axis parallel to the axis of the coils is assumed. The profiles are plotted as a function of the distance R from the axis and refer to z = 0 *mm* and z = 7.5 *mm,* i.e. to horizontal surfaces located to the middle and to the top of the ring. As it can be seen from figure 2.4.2 the magnetic field produced by the coils is nearly uniform and axial directed; a light inclination toward the inside is observed far from the axis for $z \neq 0$.

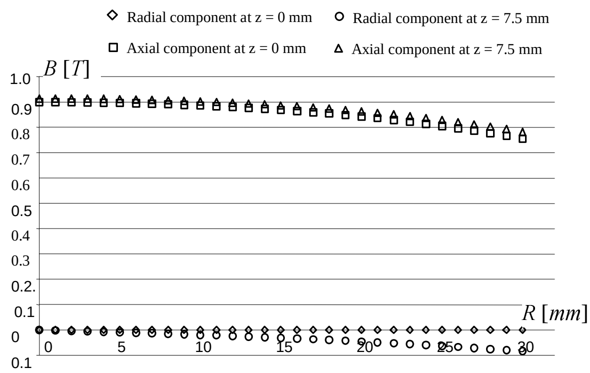

figure 2.4.2: magnetic flux density produced by the coil without SC ring at t= 3 ms

The distribution of the axial component of the magnetic flux density trapped by the ring after the application of the pulse is measured by scanning a $52 \times 52\ mm^2$ horizontal surface located at 1 mm above the ring top, by means of a mono-axial Hall sensor having an active area with 0.5 mm diameter. The measurement, performed with the sample immersed in the liquid N_2 bath, starts 240 s after the application of the pulse (a delay needed to extract the sample from the coil and locate it below scanning mechanism) and require a total time of 670 s, with a scanning step of 1 *mm* along the two directions.

The numerical calculated axial and radial components of the magnetization trapped inside the YBCO ring after the application of the field pulse are shown in figure 2.4.3. The three meshes described below are used for the calculation.

- Mesh 1, made of 160 prisms with triangular basis, arranged in 2 section of 80 prisms each; any section covers one half of the entire height of the ring.
- Mesh 2, made of 320 prisms with triangular basis, arranged in 4 section of 80 prisms each; any section covers one fourth of the entire height of the ring.
-Mesh 3, made of 392 prisms with triangular basis, arranged in 4 section of 80 prisms each; any section covers one fourth of the entire height of the ring.

The numerical results obtained by means of the three meshes are coincident, confirming that the numerical convergence is reached, both with respect to radial and the axial direction[3]. The hysteresis loop used for the calculation, measured on thin slab, is taken from Murakami [52]; the fitting parameters are B_{peak} = 0.1 T, μ_0 $M_{sat.}$ = 0.04 T, ΔB_{peak} = 0.1 T, and μ_0 M_{peak} = 0.48 T. The conventional permeability ν utilized for solving the non linear system through the fixed point technique (see equation (2.2.29)) is equal to $-1/\mu_0$.

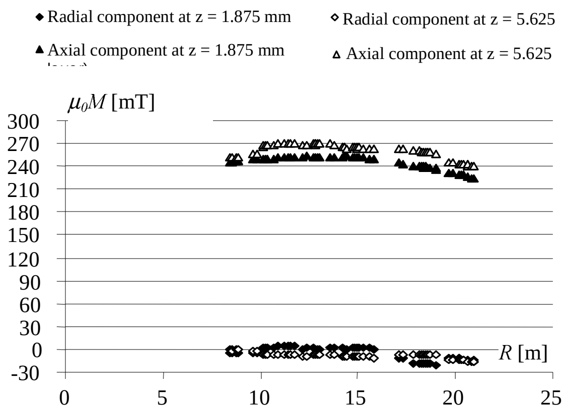

figure 2.4.3: trapped magnetization inside the YBCO ring

As it can be seen from figure 2.4.3 the calculated trapped magnetization is about axial directed; a small radial component is observed on the outer part of the ring. The azimuthal component, which is not shown in the figure, is zero everywhere. An increase of the axial component is observed along the ring height. Notice that a light increase of the axial component is observed also for the applied field (see figure 2.4.2).

There is no way to compare the numerical results of figure 2.4.3 with experimental data because the magnetization trapped inside the sample cannot be measured. However the trapped magnetization produces a certain distribution of (trapped) magnetic flux density outside the ring, which can be calculated by means of equation (2.1.18)[4]. Since the outside magnetic flux density can be measured, a comparison with

[3] The convergence is evaluated with respect to the magnetic field trapped outside the ring
[4] The first integral of equation 2.1.18 is zero because after the pulse $\mathbf{J}^{ext}$ is zero. Moreover, the second integral is convergent since we consider only points outside the ring.

experimental results is possible. Nevertheless, in case of agreement, we do confirm that our calculation well reproduces the physics outside the sample and we do not claim more, because, as largely discussed so far, what we calculate inside is prevalently a matter of modeling.

The numerical calculated axial component B_z of the magnetic flux density trapped over a surface placed a 1 *mm* distance from the top of the YBCO ring, corresponding to the magnetization distribution of figure 2.4.3, is shown in figure 2.4.4 as a function of the distance R from the ring axis. The same figure also shows the experimental plotted B_z versus R profile. The error bars represent the minimum and the maximum excursion from the average value of the measured data over a circle with radius R.

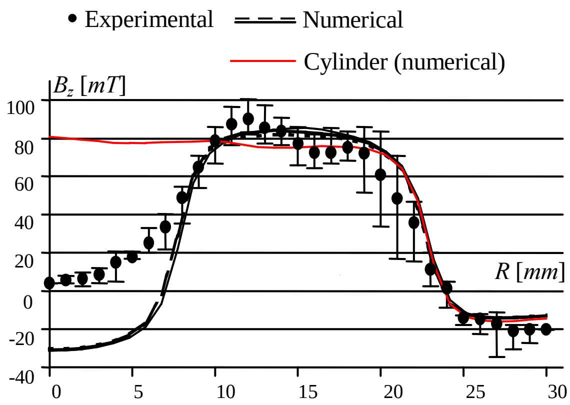

Figure 2.4.4: trapped magnetic flux density at 1 mm distance from the ring top

The numerical results of figure 2.4.4 are in a good agreement with the experimental ones as long as the field distribution over the YBCO ring surface and its outer part are concerned, whereas no correspondence exists for the field distribution over the sample hole, where the calculated field has opposite sign with respect to the experimental one. The negative sign of the numerical field in the hole could be expected, since the numerical results concerning the magnetization (see figure 2.4.3) show a nearly uniform magnetized ring.

To carry out the calculation, the hysteresis loop measured on a thin slab is assumed as constitutive relation, i.e. it is supposed to have local validity. This is a quite arbitrary move and could be at the origin of the mismatch. However, when the same constitutive relation is applied to carry out calculations on simply connected geometry, say cylinders, a good agreement between numerical and experimental results is obtained. Even though out of context, the calculated magnetic flux density trapped by a YBCO cylinder having the same radius and thickness of the considered ring and subject to the same field pulse is also shown in figure 2.4.4, in order to appreciate the qualitative agreement with experimental results [58,61].

It is clear that the numerical results for the ring sample obtained through the hysteresis curve based model are complementary with those obtained by means of a model utilizing the E-J power law as constitutive relation. Actually, we have yet observed that an E-J power law based model can hardly predict the experimental fall of the trapped magnetic field above the hole of ring shaped samples. On the other hand, an hysteresis curve based model reasonably leads to a negative field trapped in the hole. Therefore it seems that none of the two approaches can autonomously give a complete account of the experimental observation, rather, since the discrepancy is opposite in the two cases (one overestimates and the other underestimates the field in the hole) it seems reasonable to believe that the *combination* of the two modeling approaches could allow a better schematization of the superconducting behavior. Anyway, if this way is followed, i.e. the E-J power law and the hysteresis curve are both assumed as constitutive relations, it is agreed that the superconductor behaves like a conducting as well as an independently magnetizable material and the hysteresis loops cannot be any longer considered as a mere macroscopic effect of the shielding currents yet is accepted that they express also some independent feature that emerges and becomes crucial in some cases, e.g. when multiply connected geometries are considered.